

An implementation and evaluation of large-scale multi-user human–robot collaboration with head-mounted augmented reality

Xiliu Yang ^{a,e}, Felix Amtsberg ^{a,e}, Benjamin Kaiser ^{b,e}, Lior Skoury ^{c,e}, Tim Stark ^{a,e}, Simon Treml ^a, Nils Opgenorth ^a, Aimée Sousa Calepso ^{d,e}, Michael Sedlmair ^{d,e}, Thomas Wortmann ^{c,e}, Alexander Verl ^{b,e}, Achim Menges ^{a,e}

^a Institute for Computational Design and Construction (ICD), University of Stuttgart, Germany

^b Institute for Control Engineering of Machine Tools and Manufacturing Units (ISW), University of Stuttgart, Germany

^c Institute for Computational Design and Construction, Chair of Computing in Architecture (ICD-CA), University of Stuttgart, Germany

^d Visualization Research Center (VISUS), University of Stuttgart, Germany

^e Cluster of Excellence Integrative Computational Design and Construction for Architecture (IntCDC), University of Stuttgart, Germany

ARTICLE INFO

Keywords:

Human–robot collaboration
Augmented reality
Robotic fabrication
Timber prefabrication
Co-design

ABSTRACT

Human–robot collaboration (HRC) offers promising potential for more flexible and sustainable production practices in architecture and construction. This requires HRC setups to scale up from light-payload collaborative robots to conform with the scale of building construction while considering the safety and teamwork culture for workers. This research proposes a system for large-scale multi-user HRC using head-mounted augmented reality (AR) devices. To achieve this, we contribute three methods that work in conjunction: (1) an AR system that enables multiple users to share tasks and work together with robots; (2) a dynamic human task allocation engine that reacts to the changing production teams and task types; and (3) a safety zone generation and allocation method to configure human collaboration in shared space with large-scale robots. The system is evaluated using a case study of prefabricated timber cassettes combining discrete event simulations, a user study and a fabrication process demonstrator with an industry partner.

1. Introduction

In building construction, automation and robotics offer promising solutions for the productivity and labour challenges facing the industry today [1]. The off-site prefabrication sector is particularly suited to benefit from robotic automation and has seen several decades of development in this area. However, most of these applications are focused on product-based building solutions, while the batch-size-one paradigm of the broader architecture and construction market still presents many challenges for assembly-line automation due to the need for high flexibility [2]. Meanwhile, human workers, with the ability to execute a variety of tasks and react to unexpected events, continue to play a pivotal role during production.

Recent research on human–robot collaboration (HRC) in construction explores many possible reconfigurations of the fabrication design space to leverage the strengths of human and robotic actors [3,4]; shared-space HRC has been shown to achieve more flexible and efficient work processes and open new creative possibilities for design [5–8]. However, the interaction scenarios often focus on light-payload collaborative robots, which have distinctly different spatial relationships

and interactivity requirements compared to larger, high-payload (above 100 kg) robots needed for prefabrication.

To address this gap, this research develops a large-scale HRC system for robotic building prefabrication. We implement such a system using augmented reality head-mounted displays (AR HMDs) as the human–machine interface (HMI). Compared to mobile- and screen-based HMIs, HMDs augment the physical world intuitively in three-dimensions and afford hands-free interactions situated around physical referents [9,10]. To facilitate an AR-based HRC approach for building prefabrication, we outline three key requirements that motivated our design.

First, the AR interface needs to effectively present information from a highly coordinated technical system to users, i.e., craft workers, who have rich construction knowledge but limited programming skills. The interface also needs to provide support for interactions within the constraints of prefabrication, e.g., maintaining control over production speed and quality. Second, as construction environments involve teams of human workers and potentially unexpected events, the aforementioned communication and interaction requirements need to

* Corresponding author at: Institute for Computational Design and Construction (ICD), University of Stuttgart, Germany.
E-mail address: xiliu.yang@icd.uni-stuttgart.de (X. Yang).

be synchronised and adaptive to a changing environment and support the involvement of multiple workers in a team. Lastly, the system needs to cope with physical separations due to the safety requirements of heavy-payload robots. Safety design therefore must be integrated, and relevant interaction features should be provided in the AR support system.

Drawing from existing research on human–robot interaction that has contributed to these areas (communication, safety, synchronisation, and adaptation), an integration of these aspects for robotic building prefabrication is proposed. We focus particularly on timber building prefabrication due to (1) the relatively light weight of timber components, which makes them suitable for manual handling, and (2) a mature ecosystem of automation technologies that already exist in this sector [11], which makes HRC a timely and relevant topic for the community. The research questions guiding this work are summarised as follows:

1. How to provide suitable information and interaction support for collaborative robotic prefabrication using AR HMDs?
2. How to synchronise and adapt the production execution among multiple humans and industrial robots in response to dynamic factors?
3. How to integrate safety design for collaborative fabrication with heavy-payload robots?

In the following chapters, we present the methods developed and evaluate the integrated HRC system in a case study for producing prefabricated timber cassettes. The HRC system includes (1) an AR-HMD application that provides information and interaction support for humans to work alongside industrial robots, (2) a human-centred, multi-user allocation engine (worker pool) that interfaces human communication with the automated system and orchestrates the AR visualisations, (3) a safety zone generation and control method to configure HRC with large-scale robots. In addition to demonstrating the workflow in the prefabrication process of a segmented timber shell [12], we include simulation-based approaches and a user study to evaluate the system performance.

2. Related work

In this section, we provide a summary of existing work that contextualises our design decisions for large-scale HRC. We first review current approaches on safety mechanisms and human–robot task allocation, followed by a summary of AR applications in collaborative digital fabrication and the use of AR HMDs in this context.

2.1. Safe human–robot collaboration

Smaller-payload, collaborative robots (cobots) follow certain design principles to safely work simultaneously in the same workspace as humans. However, the entire robotic application, including end effectors and transported masses, must also be safe, often requiring additional safety technology. Integration of these safety systems has been presented in the field for construction tasks with cobots, e.g., Ruttico et al. demonstrated an autonomous mobile robot (payload 30 kg) for bricklaying with a dedicated safety PLC and AR visualisations of safety zones [13].

Compared to cobots, heavy-payload industrial robots present many challenges for HRC safety due to (1) significantly higher speed and mass, which result in longer stopping distances and the need for greater separation; (2) larger working envelopes, which make high-resolution tracking methods that work well in smaller spaces more prone to issues; and (3) with significantly higher kinetic energy and force, accidental contact is potentially catastrophic. As such, most HRC studies in the literature focused on cobots [14].

In recent years, many novel safety concepts have been proposed for HRC with heavy-payload robots [15,16]. However, real-world reports

Table 1
Requirements of SRMS v.s. SSM.

Safety mode	Human detection	Robot response
SRMS	Presence	Protective stop
SSM	(Change of) distance	Adapt motion

on the deployment of these concepts remain scarce. Notably, stringent regulatory standards require high engineering efforts and associated costs, as well as prolonged risk analysis and certification [17]. In the context of prefabrication, this also requires the integration of safety into early computational design and planning processes. Arents et al. reviewed existing shared-space HRC studies and found that 25% did not account for safety actions, and over 50% did not address safety standards [18]. To this end, our research demonstrates the integration of safety design based on relevant standards during the computational design and planning process.

2.1.1. Safety standards

ISO/TS 15066 specifies four types of human–robot collaborative modes: “Safety-Rated Monitored Stop” (SRMS), “Speed and Separation Monitoring” (SSM), “Hand Guiding” (HG), and “Power and Force Limiting” (PFL) [19]. Collaborative robots are designed to work in close proximity with humans under HG and PFL modes natively. In contrast, heavy-payload robots, unless equipped with safety-rated force-sensitive add-ons, are limited to interactions under SSM and SRMS. In addition, the use of HG and PFL is difficult in typical timber prefabrication processes because processes such as sawing and milling are inherently dangerous and require separation from humans. Below, we focus our attention on the last two, with a summary of system requirements in Table 1.

SRMS uses safety-rated access control to allow for human interactions, i.e., the robot stops when a person enters the collaborative workspace and maintains the protective stop. Both sensor hardware and communication networks must be safety-rated for compliant operation. SSM provides a more dynamic but also complex strategy whereby robot motions are adapted to ensure that the separation distance between human and robot (S) stays above the protective separation distance (S_p). The sensing system can be a combination of zone occupancy (e.g., sensor-monitored safety zones [20]) and operator position (e.g., computer vision [21]). A large body of work proposed enhancements on sensing and control methods to improve the performance of SSM, e.g., by fusing global LiDAR and local camera sensing, real-time adaptations based on operator positions showed a 29%–40% efficiency increase compared to an SRMS setup during HRC [22].

SSM involves high engineering efforts due to the aforementioned challenges around heavy-payload robots (2.1). Therefore, we opted for a simpler approach using SRMS based on fenceless zone occupancy tracking in this research. Similar to a previous implementation by Karagiannis et al., we use sensor-monitored work areas [20] associated with each prefabrication task for zone planning. The system is supplemented by an SSM-inspired function using AR location tracking; though this is not implemented on the safetyPLC, the AR alerts act as an operator awareness interface to prevent humans from disrupting robotic operation.

2.1.2. Design methods

Many guidelines have been proposed for the design of safe human–robot collaboration [23,24]. In heavy-payload industrial robotic applications, Bdiwi et al. proposed a categorisation of four interaction levels [25] used in a “level planner” when designing manufacturing processes; the levels then result in clusters of operation modes, which can be implemented through a dynamic finite-state machine using an enhanced set of safety states on the robotic system [16]. This approach provides a generalised framework to design collabora-

tion under safety standards, conduct risk assessments, and generate technical specifications needed for declaring conformity for industrial applications.

One important design consideration for high-variance, project-based building prefabrication is the facility layout constraints at the prefabrication site. Compared to on-site construction (fixed-position layout), robotic building prefabrication, similar to other small-batch production sites, often uses a process-based layout based around manufacturing platforms [26]. Optimal spatial distribution of work zones in a process constitutes a class of planning problems – Facility Layout Planning (FLP) – and is closely linked to the subsequent generation of safety zones. Though we do not propose any FLP approach in this research, we summarise heuristics applied during the planning process and focus on the subsequent generation and allocation of safety zones.

Existing case studies on HRC safety design are often conducted in virtual or mixed reality environments [27,28]. In practice, SRMS with access control devices is most commonly used in robotic fabrication projects. In cases where human participation is occasionally needed in the robotic work area, robots can also be run in manual mode under operator scrutiny and reduced speed. However, reports on safety details are uneven, if not rare, in research papers that involve the use of heavy-payload robots in robotic fabrication, echoing the research gap highlighted in past reviews [18]. To this end, we contribute a case study addressing the integration of safety for large-scale HRC during the design and planning of a timber cassette prefabrication project.

2.2. Human-centred multi-actor task allocation

A critical aspect of HRC design is the allocation of tasks to individual actors. In this research, we drew from a combination of skill-based, static allocation and human-centred, dynamic allocation approaches. Below, we briefly review existing literature on these methods.

2.2.1. Human–robot task allocation

Static and dynamic allocation methods in HRC respectively address the planning process prior to and during production execution [29]. Capability- or skill-based task allocation is a prominent approach [30, 31], which can be traced to Fitts' Men-Are-Better-At/Machines-Are-Better-At (MABA-MABA) list [32]. This starts by decomposing the process into individual tasks and considering the suitability of humans or robots for each task based on skill evaluations [33]. The matching process can also be automated using a suitability matrix [34], and the results can be optimised through simulation to improve productivity metrics [35].

Small lot-size production processes common in construction have high variability and are thus especially prone to unplanned events; these could cause run-time deviations that render a theoretically “optimal” sequence ineffective. Dynamic allocation allows the system to reactively or proactively adapt to such events [29]. A *proactive* approach is “led” by humans, either through explicit decisions or intent prediction [36], while a *reactive* approach relies on a central planner to respond to dynamic events, e.g., human factors [37] or performance [38].

In this research, we first apply a static allocation approach, i.e., using the payload and dexterity requirements of the prefabrication tasks to inform allocation during process planning, favouring robotic execution where possible. The relevant skills for this allocation were summarised in a conceptual framework for HRC in timber prefabrication previously [11]. Second, we apply a dynamic allocation mechanism to support humans in recovering from unplanned issues during robotic execution, discussed further in Section 3.3.3.

2.2.2. Human-centred task allocation

Research on human-centred systems advocates for designers to dispense with the idea of “*magic humans*” and actively anticipate the functions humans need to fulfil; this involves design efforts focused on supporting humans to effectively understand, decide, and act in the system [39]. In the context of task allocation, this principle calls for ensuring situation awareness and empowering humans to control the task progress, further supporting collaboration efficiency between humans and robots.

Human-centred task allocation also expands the evaluation focus from overall system productivity to social sustainability goals, e.g., cultivating skills, diversity, and well-being [40,41]. For instance, Gräßler et al. proposed an allocation method optimising for long-term skill cultivation, in addition to short-term task efficiency, by including age-related factors in the skill level representation [42]. Work allocation can also be optimised to workers’ skill profiles and personal characteristics to enhance productivity and job satisfaction [43].

In our approach, we implemented these human-centred principles by (1) incorporating a skill-matching function in the worker pool to account for diverse skill sets and individual choices in multi-user HRC, and (2) allowing flexible handling of unplanned errors through dynamic task allocation, supported by an AR system to enhance users’ situation awareness and ability to act in a complex construction process. The current implementation of dynamic allocation is a one-way process, i.e., human workers are always the recipients of the re-allocated task (see 3.3.3). In other words, the system can support task reallocation from human to human, or from robot to human, but not vice versa (from human to robot). Though a fully flexible, two-way allocation approach is highly relevant for dynamic construction environments and can meet more diverse human-centred objectives [44], it also poses high requirements for the safety and robustness of robotic online decision-making and control [29].

2.3. AR-supported collaborative construction

Flexible HRC relies heavily on an effective communication channel, which consists of both input (human-to-machine) and output (machine-to-human) pathways. AR provides a bidirectional medium and spatially anchors the content and interactions to physical objects, e.g., robots.

2.3.1. AR in HRC and digital fabrication

Suzuki et al. reviewed 460 papers on human–robot interaction using AR and proposed a taxonomy with eight dimensions, including system purpose, interaction techniques, design, and evaluation strategies [45]. All system purposes in this taxonomy, except for “increase expressiveness”, have seen numerous implementations from the construction and manufacturing domain: facilitating robotic programming [46,47], supporting real-time control including teleoperation [48], enhancing safety through visual overlays [49,50], and communicating robot intent by displaying trajectories and system status [51]. From a creative collaboration standpoint, AR also opens opportunities for interactive design during robotic fabrication [6,7,52].

In the digital fabrication community, a review by Song et al. summarised three categories of AR applications [53]: holographic instructions for assembly and fabrication [54,55], data sharing for immersive design and cyber–physical construction [56], and human–computer interaction for robotic interaction and programming [51,57]. Our AR implementation fits within several categories of these existing works — holographic instructions, supporting human–robot interaction by communicating robot intent, enhancing safety through overlays, and supporting user control of robotic processes.

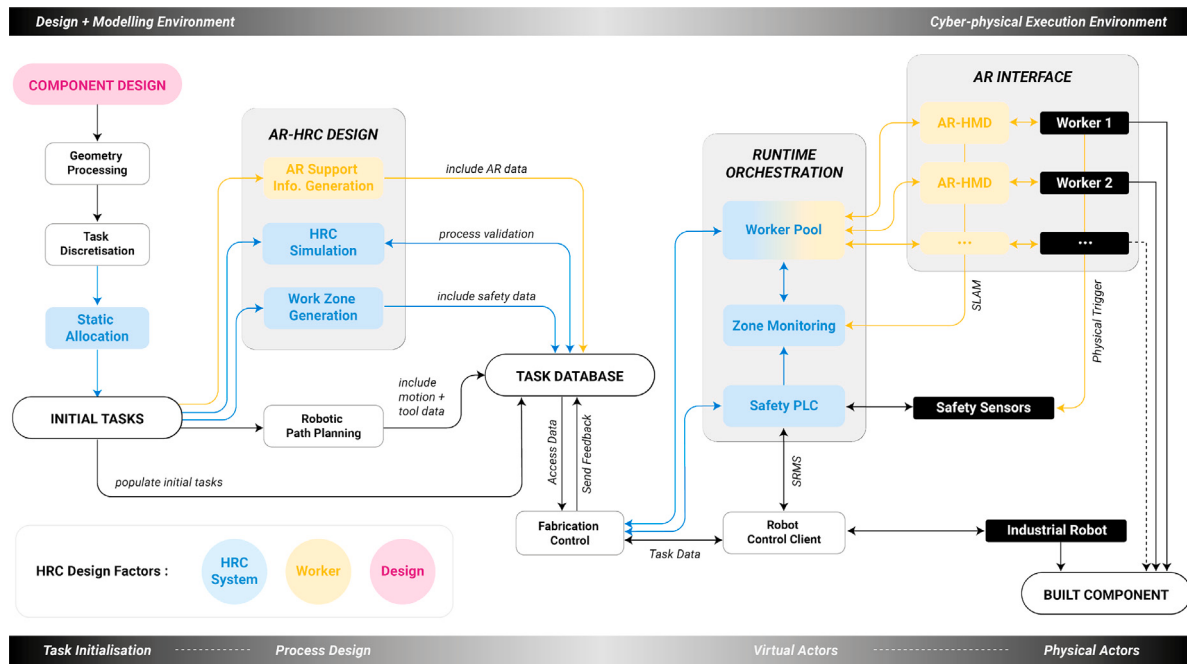


Fig. 1. The VIZOR system consists of three groups of components (1) AR-HRC Design elements that support the process design phase for computational designers, (2) Runtime Orchestration components that facilitate a safe, multi-device execution process and (3) AR Interface components that interface with the workers. Within the overall multi-actor design-to-fabrication workflow [66], the items highlighted in colours are presented in this paper.

2.3.2. Challenges and opportunities of AR HMDs

In a recent review of AR-based construction assembly studies, head-mounted displays are the most popular choice for AR visualisations [58]. AR HMDs indeed offer many advantages, e.g., rendering information in three dimensions provides unique benefits for spatial assemblies [54]. Compared to mobile- or tablet-based AR, spatial AR (projectors and HMDs) has shown higher task efficiency in comparative studies [59]. HMDs additionally offer hands-free interaction possibilities, e.g., gaze-based interaction [60], such that users can remain engaged in bi-manual physical tasks while interacting with content.

Nevertheless, HMDs still have many issues, such as a limited field-of-view and ergonomic strains when worn over longer periods. These drawbacks are shown by many empirical findings from the literature. Hietanen et al. for instance, compared projection and HMDs (HoloLens 1) for safety zone visualisations and found that the projection variant led to faster task execution and was perceived more favourably by users [50]. These issues have dwindled with newer generations of HMDs — Chan et al. compared HMDs (HoloLens 2) against joystick control in carbon-fibre composite manufacturing and found that the AR variant resulted in faster task execution and higher robot utilisation, though the joystick was perceived to be more dependable [61].

HoloLens 2 improved on many ergonomic aspects compared to the first-generation device, e.g., increased diagonal field-of-view (from 30 to 52 degrees), lighter and more balanced weight (from 579 to 566 g and moving the battery pack to the back of the headset) and more powerful computing resources to ensure a smoother experience (from 2 to 4 GB RAM) [62,63]. In the field, an identical application running on HoloLens 1 and 2 has shown a 25% increase in projection accuracy [64].

In this research, we chose to work with HMDs for the benefits above and the optimism that as technologies improve, users' perception and trust in using such systems will likely rise alike. We also build upon our ongoing investigations in large-scale HRC through AR HMDs, where this implementation addresses two issues highlighted in a previous exploratory user study: the need for non-dyadic communication support and integration of safety systems [65].

3. Methods

In the following sections, we give an overview of the workflow and architecture, before we detail the three methods to support multi-user, large-scale HRC in prefabrication, including (1) the AR-HMD system, (2) the worker pool, and (3) the safety zone system.

3.1. Workflow and architecture

A diagram of the overall system is shown in Fig. 1, where the methods presented in this paper are highlighted in colours and grouped in three clusters based on the phase of the application.

3.1.1. Design + modelling

The HRC workflow is initialised by the generation and configuration of collaborative tasks in a digital modelling environment. During this process, the building components and the corresponding geometries are converted to discrete fabrication tasks. Static task allocation decisions are made based on payload and dexterity requirements of each task and favour robotic execution where possible [8]. This preliminary task list then informs the design of the safety zones in a process described in Section 3.4.

These task data are stored as a series of *task objects* in a cloud database, which allows modifications when designing details of the fabrication procedure. Such details include digital instructions for individual actors, e.g., path planning and code generation for robots, and AR information and safety data for human participation. A Grasshopper plugin [67] facilitates the generation of AR information and work zones, which are then embedded in the task definitions (Section 3.2).

3.1.2. Cyber-physical execution

Before physical execution, the relevant tasks are accessed by a fabrication control system and stored locally to avoid latencies due to internet connection. The control system manages the execution of tasks by extracting, formatting, and supplying this data to each actor and monitoring their progress [66]. Individual control interfaces for different physical actors are implemented as virtual actors, which serve

Table 2

Summary of AR information provided in the VIZOR interface. The reference scale for levels of automation can be found in [11]. (MRTK = Mixed Reality Tool Kit, which provides SLAM and hand tracking on the HoloLens 2 HMD device.)

Visualisation type	Task level of automation			Referent	
	Category	LoA_{cog}	LoA_{phy}	Physical object	Tracking
Task geometry	I,II	[2,5]	[1,5]	Workpiece or Robotic platform	QR code
Robot trajectory	I	[4,5]	[4,5]	Robotic platform	QR code
Task instruction	II	[2,3]	[1,2]	Workpiece or Hand/Head	QR code/MRTK
Task list	III	[1,2]	[1,2]	Hand/Head	MRTK
Safety information	I, II, III	[1,5]	[1,5]	Robotic platform or Head	QR code/MRTK

as moderators between the control system and the physical actors [68]. For industrial robots, this involves motion control implemented either using proprietary protocols, e.g., EthernetKRL [69], or open-source systems, e.g., ROS [70]. Human actors are moderated by the *Worker Pool*, which interfaces with a “pool” of AR devices. This orchestration layer deals with dynamic factors in the work team, e.g., requesting help from each other, allocating tasks based on each individual’s skill sets, which are detailed in Section 3.3.

Each task contains zone occupancy information, which is forwarded from the pool to a zone monitoring node (Section 3.4). This node receives live locations of each user from the HoloLens SLAM tracking system and keeps track of the current danger zones to alert humans when they approach such areas. In parallel, safety control integration on the PLC receives the zone data from the control system to activate/deactivate sensors guarding each zone as required. When humans enter a guarded zone, SRMS is triggered, and the robot stops.

One technical design consideration of the worker pool and zone monitoring node is to manage safety and interactions *off-device* from the HoloLens. Minimising computations on the HMDs prolongs battery life and improves the AR runtime performance, e.g., tracking stability and interaction latency. The AR-HMD application is thus designed to display data with a more lightweight logic (Section 3.2) to improve the flexibility for deploying the application without recompilation between projects.

3.2. AR system

The AR interface provides workers with information support during the prefabrication process and enables them to interact with the fabrication process.

3.2.1. Information needs based on task LoA

HRC inherently involves adaptive Levels of Automation (LoA) for different work steps, which have both physical and cognitive dimensions [71]. We consider the information needs and interactivity for collaboration using a LoA reference scale designed for timber prefabrication tasks [11].

I: Robotic Task ($LoA_{cog} \in \{4,5\}$, $LoA_{phy} \in \{4,5\}$) When the task is physically executed by the robot in automatic mode ($LoA_{phy} = 5$) or in manual mode ($LoA_{phy} = 4$), humans either are not needed in the case of a fully autonomous system ($LoA_{cog} = 5$) or, more often, need to supervise the process in anticipation of potential issues ($LoA_{cog} = 4$). In this situation, knowledge of the robot’s current tasks and motions is useful for monitoring.

II: Manual Task ($LoA_{cog} \in \{2,3\}$, $LoA_{phy} \in \{1,2\}$) When the task is physically executed by the human, the cognitive automation level is mostly constrained in prefabrication to *Action Selection* ($LoA_{cog} = 2$) or *Intervention* ($LoA_{cog} = 3$) because the construction outcome is predetermined. This commonly uses *Manual* power ($LoA_{phy} = 1$) or *Hand-held Power Tools* ($LoA_{phy} = 2$). When the worker needs to focus on the task at hand, AR visualisations can provide in-situ guidance, but detailed visualisations of the robotic systems are likely not necessary. Safety information, however, is still needed.

III: Impromptu Task ($LoA_{cog} \in \{1,2\}$, $LoA_{phy} \in \{1,2\}$) When humans have higher cognitive autonomy to decide on actions, either

with full creative control ($LoA_{cog} = 1$) or under some degree of system constraints ($LoA_{cog} = 2$), we consider this an impromptu or improvisational task. One example is when a failed robotic task needs to be repeated under unforeseeable conditions that require a creative solution (a broken component that needs to be detached and reassembled). In this case, a more complete understanding of the overall task goals for past and future tasks and an option to collaborate with each other on a solution should be available.

Type III tasks can also include $LoA_{phy} \in \{3,4,5\}$ in case online robotic programming or teaching-by-demonstration is possible. Since this would require additional safety precautions, we leave this option out of scope for this research.

3.2.2. Task-based AR visualisation

The information needs summarised above are then translated to our implementations of the AR system with five groups of visualisations, summarised in Table 2. A screen capture from the HoloLens in Fig. 2 provides a visual illustration. The visualisation messages are modelled in Rhino and Grasshopper [67], then added to the task objects, and subsequently sent from the worker pool to be rendered on the HoloLens 2 with the respective task.

Robot Trajectory (I): The trajectories of the robot are programmed offline and can be monitored by the robotic operator during execution. They can either be shown in static form as a trajectory path or using a simulated animation (Fig. 2 ●). Both remain anchored to the robotic platforms.

Task Instructions (II): For a manual task step, the interface can inform *where* to carry out an operation, *what* to do at this location, and instructive content to indicate *how* to carry out the action. The last element is especially useful for training workers in the first few iterations of the task. These instructions are shown in addition to task geometries and could contain text and images on the holographic UI (Fig. 2 ●).

Task Geometry (I, II): The current task information can be conveyed using 3D geometries to either provide manual task guidance or provide context to support process monitoring (Fig. 2 ●). Depending on whether the task is manual or robotic, such content is either attached to the workpiece (manual tasks) or attached to the robotic end-effectors (robotic tasks).

Task Lists (III): This interface provides access to the current state of the HRC system — what tasks are being executed and what is coming up next. It gives a general overview of the fabrication process. If changes are needed to the task list at run time, e.g., reassignment, the interface should also support these actions. The panel is dynamically accessible by the user and hidden when not necessary (Fig. 2 ●).

Safety Information (I, II, III): Safety information is critical for heavy-payload robots in a fenceless setting. This is shown as highlighted areas where humans cannot enter (based on the current robotic task) and anchored to the robotic platforms (Fig. 2 ●). For dynamically triggered information, such as audio alerts and pop-ups emitted when humans approach the boundaries, the alerts are anchored to the user.

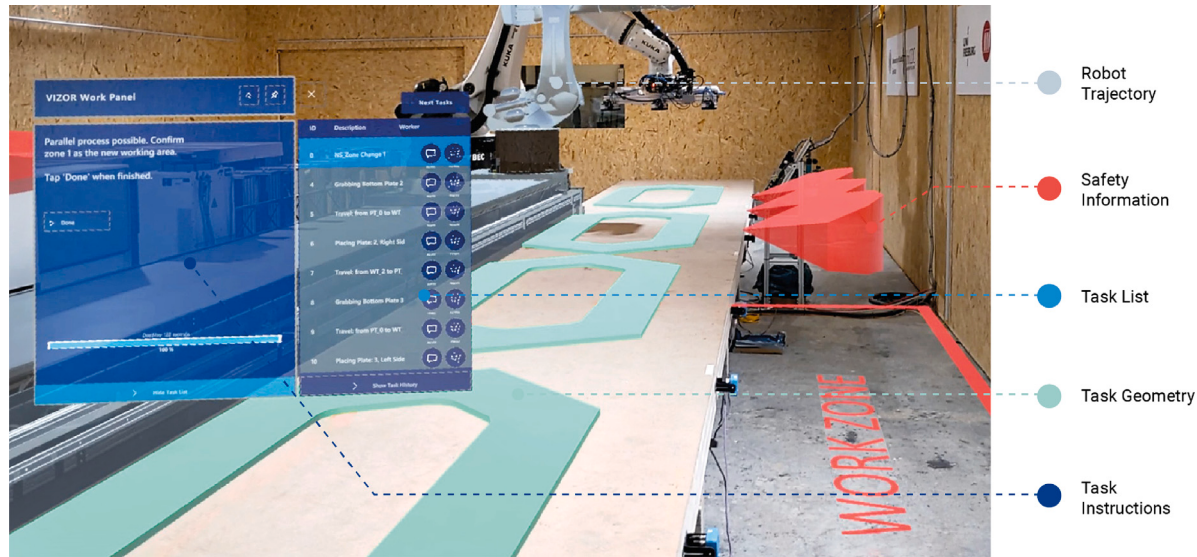


Fig. 2. Annotated AR-HMD interface captured from HoloLens 2.

3.2.3. AR interactions through the UI

In addition to rendering visualisations, AR headsets also enable workers to interact with various elements of the production system. We defined three types of interactions, implemented as UI elements (e.g., buttons, banners, sounds) tethered to a task panel, which the user can call up with their hands as they move around the workspace or set to “follow-me” to always have it 1.2 m away from head position.

Task: During manual tasks (II), workers mainly interact with physical objects in the world, and holographic instructions provide assistance. The task geometries on the workpiece and the UI panel containing task instructions are automatically triggered when the AR device receives the task. To synchronise these human tasks with the digital fabrication system, the user signals task completion with a *Done* button on the UI panel and can optionally *Reject* a task, e.g., when it is not feasible.

Team: With multiple users participating in a task sequence, the AR-HMD provides two communication features for interacting within the team: an automatic *notification* that signals individual task completion on one device to others in the work team, and a *help* button to request assistance from another teammate.

Process: To make use of the construction experience and knowledge of the workers during fabrication, the interface also provides a means to intervene in the robotic process when necessary. The task list provides the sequencing information to support these decisions, where past and upcoming tasks can be queried and viewed. Reassignment is possible through a button next to each list item, i.e., from a robot to a human or vice versa.

3.3. Worker pool

The aforementioned visualisation and interaction functions are supported by a coordination mechanism – “*worker pool*”, which communicates with multiple AR devices through a publisher-subscriber network using the ROS protocol. The pool, on the one hand, interfaces multiple workers with the fabrication control system and, on the other hand, manages the updates of AR visualisations to minimise computations on the HMDs. We describe below the implementation of the worker pool, which stores the following variables:

- W : Set of all workers in the pool
- $S(w)$: Skill parameter of worker $w \in W$
- $Available(w)$: Availability of worker $w \in W$
- $Team(\tau) \subseteq W$: The team assigned to task τ

- T_P : Set of all tasks in the priority queue
- T_N : Set of all tasks in the non-priority queue
- A : Hash map of active tasks for the worker pool, with team-task pairs $f_a : Team(\tau) \rightarrow \tau$
- P : Hash map of passive tasks for execution by other actors, with actor-task pairs $f_p : \alpha \rightarrow \tau$

3.3.1. Task processing

When the worker pool receives a task from the fabrication control system [69], it first checks whether it targets manual or robotic execution. If the task is assigned to humans, it is added to a first-in-first-out task queue, T_P or T_N , depending on whether the task has priority. These two queues act as buffers to isolate the incoming tasks from actor executions, making more dynamic interactions between AR devices and the pool possible. Each task has a sequential or parallel designation. If the task is parallel, the pool immediately requests the next task from the server, allowing multiple actors to carry out tasks simultaneously without blocking.

If the task is aimed at robotic execution, the task object is stored with the executing actor as the key in a hash map of “passive” tasks P :

$$P \cup f_p : \alpha \rightarrow \tau \quad (1)$$

Information related to this task is also immediately converted to AR visualisations and sent to all active workers as described in 3.2.2. It includes the current safety area, work geometries that the robot will manipulate, and, if necessary, a simulation of the robotic trajectory.

3.3.2. Human-centred task allocation

If the task is aimed at manual execution, it is allocated to AR workers in a background routine using the two queues. This allocation decision adapts to explicit user choices for each worker w using a skill parameter $S(w)$, where the matching logic from a task τ to the available skill is preconfigured in $Match(S(\tau), S(w))$. This pre-configured matching function can be extended to incorporate models that account for human factors issues, e.g., learning curve models [42], that allow the function to consider dynamic skill level adjustments during runtime.

At the start of the allocation process, a task object is retrieved from the relevant task queue (T_P before T_N), and an empty list $Team(\tau)$ is created. The pool then iterates through the workers following the selection criteria:

$$Team(\tau) \cup \{w \mid Available(w) \wedge Match(S(\tau), S(w))\} \quad (2)$$

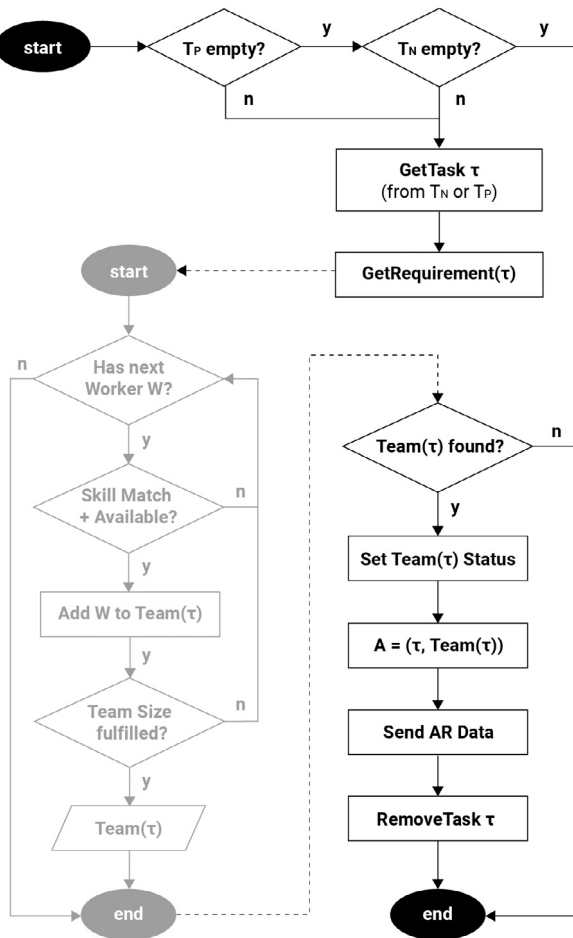


Fig. 3. Task allocation flowchart. Black denotes an outer loop that processes tasks in the queue. Grey denotes an inner loop that allocates the workers for the task.

This selection mechanism allows the task assignment to consider the work team's unique skills, experiences, and potential user preferences. If $|\text{Team}(\tau)| < \text{Required}(\tau)$ at the end of the iteration, the allocation routine restarts. If a team of sufficient size is found, the task instructions are sent to each worker, and the availability is updated $\forall w \in \text{Team}(\tau) : \text{Available}(w) \leftarrow 0$ for the team. The task object is then stored in a hash map of active tasks A :

$$A \cup f_a : \text{Team}(\tau) \rightarrow \tau \quad (3)$$

Task completion requires all allocated team members to respond with a success message, i.e., by the user clicking the “Done” button on the AR interface, which sets $\text{Available}(w) \leftarrow 1$. When all members of a team become available, we remove the task from the current map of active tasks:

$$A \setminus \{f_a : \text{Team}(\tau) \rightarrow \tau \mid \forall w \in \text{Team}(\tau), \text{Available}(w)\} \quad (4)$$

A summary of the allocation loop is depicted in Fig. 3. One important note is that the implementation above relies on *proactive* human action for effective allocation, which has an important implication for human factors. For instance, a worker can mark an erroneously executed task as correct, or a worker can repeatedly fail tasks but not modify their skill setting. These situations can occur in practice, e.g., due to fatigue, and would require system-initiated assurance measures, e.g., error checking or raising alerts. We further discuss system designs that can mitigate these issues in the outlook.

3.3.3. Adaptation and recovery

The worker pool uses the priority T_P to adapt to unplanned events during fabrication. Extending from previous case studies [8], we primarily consider three types of events that may occur during production.

First, the operator may manually abort the robotic process, or the system may return an error during execution. When the pool receives the failure status message from actor α , it removes task τ from the passive tasks P and adds it to the priority queue, i.e., the failed task is allocated to the work team with priority:

$$T_P \cup \{\tau \leftarrow P[\alpha] \mid \neg \text{Success}(\alpha)\} \quad (5)$$

Second, a human worker may not be able to complete a task, which can be handled in two ways. If the human interacts with a “reject” button, i.e., the pool receives the status message $\neg \text{Success}(w)$, the task is reallocated through T_P , similar to (5). Alternatively, the task information can be shared with another member of the team without reallocation. In this case, the user interacts with a “Help” button. All active devices receive the assistance request as a popup message with data on the worker requesting help, w_{req} . When a user chooses to accept the request, they click “Accept” and the HMD sends the following response to the pool (w_{req}, w). The pool retrieves the task information and shares it with the requesting worker:

$$\tau \leftarrow f_a(\text{Team}(\tau) \mid w_{req} \in \text{Team}(\tau)) \quad (6)$$

Lastly, a user can explicitly reassign a task ahead of time. When a reassignment request is made from a device, the request is sent to the fabrication task control system. The worker pool then receives a response from the server containing the tuple (τ, α^*) . If the reassignment is successful ($\alpha^* \neq \emptyset$), the pool triggers a task list update in all AR devices. In both the first and third cases where a robotic task is taken over by humans, the associated safety zones are deactivated to allow for manual execution.

3.4. Safety zone integration

The task-based safety zone integration provides the infrastructure to ensure the collaborative task flow outlined above can occur safely. This consists of zone segmentation based on the layout design, zone selection and embedding in robotic tasks, conversion to safety sensor layouts, and hardware connections and configuration on the PLC and controller. In the following paragraphs, we present a method to generate, optimise, and associate zone definitions for human–robot collaboration using a process illustrated in Fig. 4, followed by a description of physical implementation through sensors and PLCs.

3.4.1. Layout types and heuristics

Though the number and size of safety zones roughly scale to the reachable areas of the robot, they also closely relate to the building component being fabricated. We distinguish between three types of layout strategies based on the relationship between the building component (BC) and robotic reach (RR):

- $BC > RR$: If the component's global geometry exceeds the robot's reach, local geometric features within the component need to be clustered for each execution stage, followed by manual workpiece transportation between stages. The internal geometries have a high impact on zone segmentation, as seen in the project from [69].
- $BC \approx RR$: For components with a similar size as the robot's reach, the zone segmentation is directly based on robot reachability. Capability maps can inform this process [72]. In the case of a robot mounted on a stationary base, the most frequent solution is a radial arrangement around the robot, as seen in the project from [26].

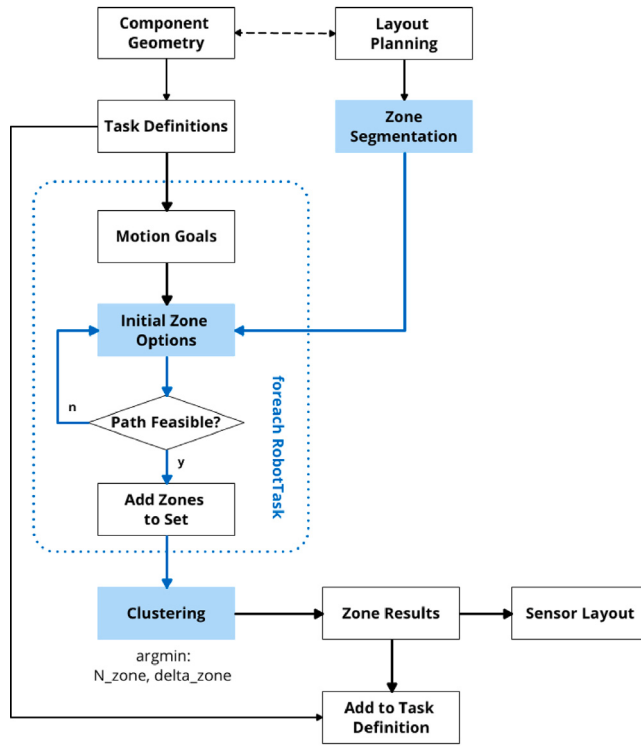


Fig. 4. Work zone generation flowchart.

- $BC < RR$: For components much smaller than the full reach of the robotic system, multiple elements can be arrayed in the workspace and batched to improve efficiency. The array of these elements determines the zone segmentation. An example of this layout is the case study we use later on.

The overall facility layout, including initial positions and sizes of the equipment and assembly stations, is often co-designed with the relevant industry partners. In the scope of this paper, this information is considered an a priori input to the zone generation steps that follow.

3.4.2. Work zone generation

The aim of the work zone generation process is to find for each robotic task τ an optimal zone constraint $Z(\tau)^*$ to maximise the spatial flexibility of designing human tasks for parallel execution.

Given the defined positions and sizes of equipment and assembly stations, we simplify the initial zone segmentation by constraining each zone to have rectilinear borders and iteratively placing the largest cell until the workspace is full. The output is an initial graph structure G containing a set of safety zones Z as nodes and the adjacency of zones as edges.

- Z : Set of all zones in the workspace.
- $Z(\tau)$: One set of viable zone constraints for task τ .
- $\zeta(\tau)$: All sets of viable zone constraints for task τ .

The task definitions are then used to extract motion goals, providing a set of zones that must be reached for a given task, e.g., a robotic pick and place task may have $Z_R(\tau) = \{z_{\text{Pick}}, z_{\text{Place}}\}$. The trajectory linking the required zones passes through a series of possible zones $Z(\tau)$, which can be found using a depth-first search in the zone graph. However, some of these solutions will contain circuitous paths, which are undesirable in production, and can be filtered with a preset maximum zone count per task (C_{\max}).

$$\zeta(\tau) = \{Z(\tau) \in DFS(G, Z_R(\tau)) \mid |Z(\tau)| \leq C_{\max}\} \quad (7)$$

The filtered $Z(\tau)$ can then be verified using a motion planning pipeline (e.g., MoveIt) to check for path feasibility based on the robot kinematics model, end-effector and environment collision geometries. Only the viable zone constraints are added to the final set $\zeta(\tau)$, i.e. where reasonable and collision-free paths are feasible:

$$\zeta(\tau) = \{Z(\tau) \mid Plan(Z(\tau), \tau) = \text{Success}\} \quad (8)$$

Lastly, we optimise the robotic paths and zone usage in the set $\zeta(\tau)$ to minimise the number of zones occupied and the number of zone changes between sets. The relative importance of the first objective compared to the second can be weighted by a parameter (λ). Additionally, each zone can also be given weights to prioritise certain zones to remain free, e.g., zones where manual tasks are dense, or vice versa, e.g., zones that are occupied by end-effector stations.

$$Z(\tau)^* = \operatorname{argmin}_{\tau_i \in T} \sum |Z(\tau_i) \Delta Z(\tau_{i+1})| + \lambda |Z(\tau_i)| \quad (9)$$

We use a dynamic programming approach to iterate through the tasks with associated zones and solve for the optimal zone set $Z(\tau)^*$. Generating this work zone information provides the constraints to design human task execution safely, i.e., only using the zones which are free.

3.4.3. Physical configuration

The robot controller and safety sensors must be configured to monitor all hazard zones. With SRMS, it is necessary for a human entering the danger zone to trigger an emergency stop of the robot. Safe sensor systems based on various measurement principles, such as lasers, light barriers, or radar, can be used to safeguard these hazard areas. The sensors must be connected to the safety PLC, and the arrangement of the sensors must safeguard the hazard zones in accordance with the relevant standards.

Common robot controllers from various manufacturers also offer advanced safety features that enable safe monitoring of the Cartesian workspace, e.g., FANUC's Dual Check Safety (DCS) and KUKA's Safe Operation, which can define up to 16 rectangular Cartesian work areas constraining its motion [73]. The bounding volume of the robot geometry and end effectors is additionally defined using spheres. The individual Cartesian constraints can be activated or deactivated via safe outputs of the safety PLC. This makes it possible to include the previously defined work zones in these Cartesian workspace constraints.

The geometric relationship between work zones, Cartesian constraints and the protective fields used to protect the danger zones is established during setup. If a work zone needs to be accessed by humans, the safety sensors in that area are muted, and the corresponding Cartesian work area restrictions are activated instead, preventing the robot from entering the work zone. Ensuring that the Cartesian work area restrictions are linked to each task provides additional redundancy to the safety system.

3.4.4. AR safety zone monitoring

In addition to the safety zones configured through the PLC, we included a “warning” zone, defined with a 2 m offset from the “danger” zones. The offset can be reconfigured based on the robot’s operating speed and the resulting stopping distance. The differences between the two zones are:

- **Danger Zone**: sensor-guarded limits which, upon entry, the safety PLC stops the robotic task, i.e., SRMS. The zone is considered active when the safety sensors are activated on the PLC (reaction time: e.g., ≤ 100 ms [74]).
- **Warning Zone**: soft limits which, upon entry, the AR system emits an alert informing the human to move away from the area. The zone is triggered using SLAM tracking on the HoloLens (reaction time: e.g., 500 ms, based on programming).

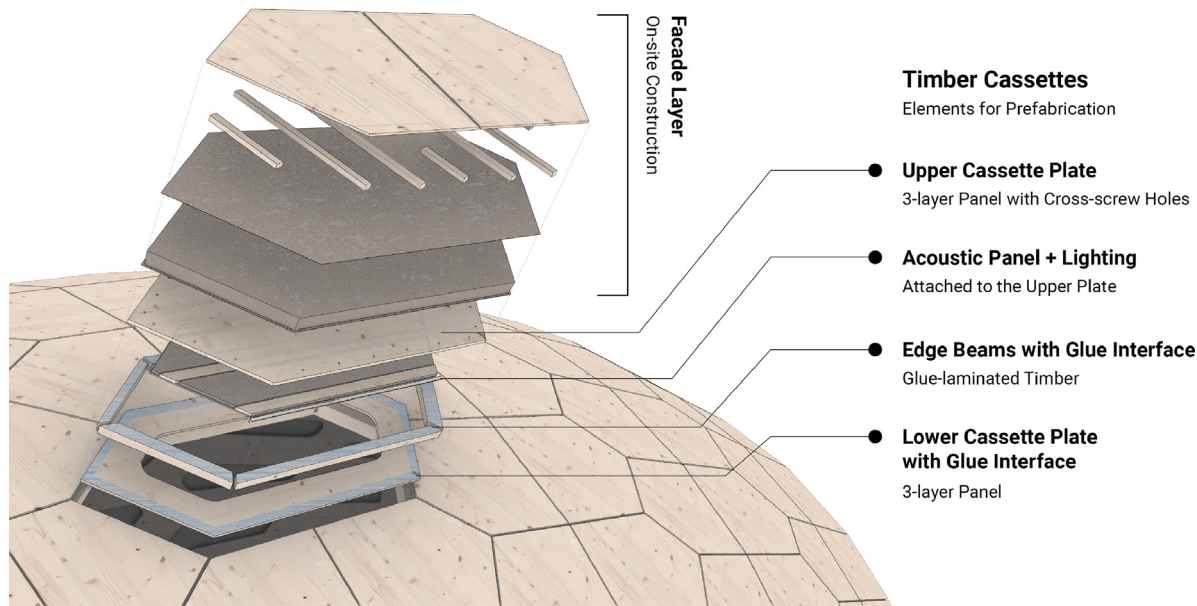


Fig. 5. Elements for prefabrication in the livMatS Biomimetic Shell.

This, on the one hand, minimises potential disruption of robotic processes by pre-empting workers from moving close to sensor-guarded areas, and on the other hand, helps humans stay out of areas that are theoretically safe but may be too close to the robot's motion trajectory and cause psychological discomfort. For applications where psychological comfort is essential, further calculations on the separation distance can be used to reduce the robot's speed (SSM) when warning zones are triggered. The hard limits are displayed in boundary lines.

A zone monitoring node in the system checks the current robotic zone against the human position at a frequency of 2 Hz. If the human enters the *warning* zone, an alert repeatedly appears in front of the user (every 1.5 s). Since entering the *danger* zone requires the operator to restart the robot after stopping, the soft limits further help to prevent unwanted disruptions, which are detrimental to time-critical processes such as adhesive applications.

4. Case study

The methods described above were applied and tested in a case study for the prefabrication of timber cassettes. In this section, we first introduce the project setting and demonstrate the workflow for HRC planning.

This is followed by two evaluations which were conducted outside of the live production runs: (1) discrete event simulation, focusing on the production performance metrics as a result of various parameters of multi-user HRC, and (2) a user study, focusing on the experience of carpenters and their qualitative feedback on the interface and interactions. Lastly, we describe the physical implementation demonstrated over three production batches of prefabrication tasks at müllerblaustein Holzbauwerke GmbH, a timber construction company in southern Germany.

4.1. Project background

The Living, Adaptive and Energy-autonomous Materials Systems (livMatS) Biomimetic Shell is an extension of the FIT Center for Interactive Materials and Bioinspired Technologies at the University of Freiburg. It is a segmented timber shell structure inspired by sea urchin skeletons. This lightweight timber construction spans a floor area of 200 m², with a free span of 16.5 m, and is composed of 127 uniquely shaped hollow cassettes, each 14 cm thick [12].

The lightweight cassette system comprises upper and lower layers of three-layer spruce boards and spruce edge beams, customised in size according to local load requirements. These cassettes serve as the primary load-bearing structure and incorporate integrated acoustic panels and lighting elements. They are prefabricated off-site and assembled on-site using cross-screwed joints, creating a form-active structure.

This research demonstrator provided a unique opportunity to serve as a case study for the HRC system for two reasons. First, the electrical components in the cassettes required manual installation; this meant that human tasks needed to be synchronised in between robotic assembly steps. Second, the project was the first initiative to use the newly developed robotic prefabrication platforms, which enabled the parallel assembly of four cassettes with a 13 m long workspace around the heavy-payload industrial robot. This required a flexible and large-scale HRC setup.

4.2. Static task allocation

The initial task sequence is generated based on the geometry of the timber cassettes. Each timber cassette consists of building elements such as beams, bottom plates, and top plates, as shown in Fig. 5. The main robotic actor is a 7-axis robot platform (KUKA KR420-R3330 mounted on a 10.7 m long linear axis). A quick-change system at the flange of the robotic arm supports four different end-effectors: a large vacuum gripper for plates, a small vacuum gripper combined with a nail gun for gripping and fixing beams, a glue end-effector for adhesive application, and a spindle for all subtractive manufacturing steps. The human workers at the prefabrication site are a combination of digital fabrication researchers and carpenters from the industry partner.

The HRC planning process starts with the initial static allocation of actors to the cassette assembly tasks based on skill considerations. Picking and placing the timber plates and beams, as well as gluing, nailing, and subsequent milling operations, require high precision and payload, for which robotic automation is more suitable and efficient. The cassettes contain embedded electrical components, which require dexterous manipulations of thinner materials (LED strips and wires) and manual checking that the circuits are operational before the cassettes are closed. These tasks are executed by humans prior to the gluing of the beams and the placing of the top plates. Due to the need for moisture control in the timber beams for glue adhesion, the beam magazine also needs to be loaded by humans shortly before robotic pick-and-place. This initial task list with actor assignments informs the subsequent process design steps.

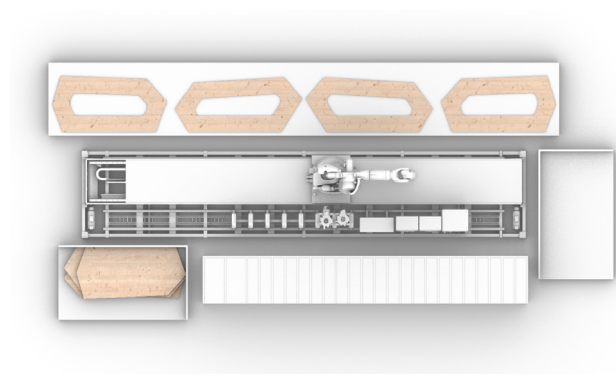


Fig. 6. Fabrication layout.

4.3. Prefabrication layout

At the centre of the prefabrication workspace was a newly developed, transportable 7-axis robotic platform, capable of fabricating four elements up to 3.5 metres in length. The work area also needed to include a work table for assembling the cassettes, multiple stationary and movable material input/output stations for plates and beams, tool stations for storing the end effectors, a milling cutter station, and a gluing machine. All these components were housed within a cell monitored by a safety system with operable doors, ensuring dust protection during subtractive processes and maintaining worker safety. As shown in Fig. 6, the robotic platform was centrally located, with material stations arranged radially around the linear platform for robotic access.

An analysis of the required process and tasks was used to address the spatial and functional demands of the robotic systems. Collaborative workshops with engineers and planners from the research team and the partnering wood construction company facilitated requirement gathering, focusing on operational needs and spatial constraints. For instance, the cell needed to be integrated within a larger fabrication hall. Some material stations needed to be accessible by crane, forklift, or cart for efficient material feeding without interfering with other projects. This process of negotiating the reachable robotic space and external requirements from individual production sites can be similarly applied to robotic systems with alternative form factors, e.g., robots mounted on a 2D gantry instead of a 1D linear axis.

Leveraging empirical knowledge, different stations were arranged around the central robot to ensure workflow efficiency and ease of access. During the conceptual phase, boundary conditions and edge cases were simulated using the VirtualRobot Plugin for Rhino3d/Grasshopper. This process allowed for the pre-verification of layout and reachability, as well as the generation of geometric requirements necessary for effector development. The layout maximised available space in the hall, with clear entry and exit points for material supply and worker movement.

4.4. Safety zone generation

The layout design described above is represented in a 3D model specifying the positioning of the robotic platform and various material input/output stations. The initial segmentations (Z) based on these inputs are illustrated in Fig. 7. Option A contains 10 zones, but due to the low width of a single cassette zone, we included a simplified segmentation option B by collapsing two cassettes into one zone, resulting in 8 zones (Fig. 7b).

The motion goals from each robotic task in the task list are converted to a list of tuples containing the target zone numbers in each task, e.g., for picking up from material supply zone to cassette number 3, in zone graph A would be $Z_R = \{4, 3\}$ and $Z_R = \{4, 2\}$ in graph B. We then sample the possible paths between these required zones filtered

by an upper limit C_{max} . Results of this sampling process are illustrated in Fig. 7a1 and b1 respectively. With a maximum of 4 zones per task ($C_{max} = 4$), the sampling process returned an average of 4.8 solutions for each motion with a standard deviation of 1.99.

The feasibility check is then run through the MoveIt pipeline using the Pilz industrial motion planner, and the remaining feasible zones are optimised based on the objective laid out in Eq. (9). The optimal results for segmentation A and B are shown respectively in Fig. 7a2 and b2. Assigning $\lambda = 1.0$ takes into account the preference for occupying as few zones as possible; compared to the alternative assignment where $\lambda = 0.0$, the latter occupied more zones that are not strictly necessary for the task.

The subsequent sensor configuration was based on segmentation B. The free zones are then used for designing human tasks in parallel, and the final fabrication task and zone occupancy map for HRC are shown in Fig. 8. The robot always occupies zone 7, whereas zones 1, 2, and 6 require access control to coordinate safe entries by the humans. The zones assigned to each human task are inserted into the relevant *task objects*, and the PLC tasks that modify the monitored zones and Cartesian constraints are added to the task list.

4.5. Safety sensor configuration

Following the zone definitions, the safety sensors are installed. The safety sensors used in this implementation are safe radar sensors (Inspect LBK-S01) with a guaranteed reaction time of ≤ 100 ms and safety integrity level 2 [74]. The sensors have a range of up to 4.00 m. The sensor area can be configured with a horizontal aperture angle of either 110° or 50° and a vertical aperture angle of either 30° or 15°. This allows adaptations to the specific working environment. The effective range can be categorised into two fields: warning fields and protective fields. Warning zones are used to slow down the robot when activated, while protective zones cause a safety stop. The sensors also allow automatic resumption of movement when the protective field and danger zone are cleared.

A total of 12 sensors are installed at different workstations around the robotic platform, covering the various work zones described above, and are connected to the safety controllers via CANopen. Each safety controller can handle up to 6 sensors, which means that each platform has two safety controllers connected to the PLC that runs the safety program using ProfiSAFE. The physical layout of the sensors is shown in Fig. 8 with a horizontal cone angle of 110 degrees. When human movement triggers the sensor fields, the reaction speed is guaranteed by the industrially certified sensor and PLC protocol; we report no perceivable latency in the field.

4.6. Task instruction detailing

The exact task instructions for each actor are then detailed by different members of the project team. For robotic tasks, fabrication data, such as tool frames, are generated within the design model and then oriented in the specified fabrication environment. Each task is digitally simulated using the VirtualRobot plugin in Grasshopper to check for reachability and collisions. The frame represents the target position for the Tool Centre Point (TCP) of the robotic end effector. The target frame's position is used to calculate the robot's overall position and the individual axis values through inverse kinematics. Each axis is then verified to ensure it remains within its physical movement range, preventing singularities and potential fabrication interruptions. Along with additional task information like offset and speed values, this data is used to parametrise robotic skills implemented in KUKA robot language (KRL).

The human task instructions are generated similarly based on the design model. For the LED installation task, the lighting elements and respective labels are converted to geometry messages in a coordinate system with the robotic platform as the origin. For the task of loading

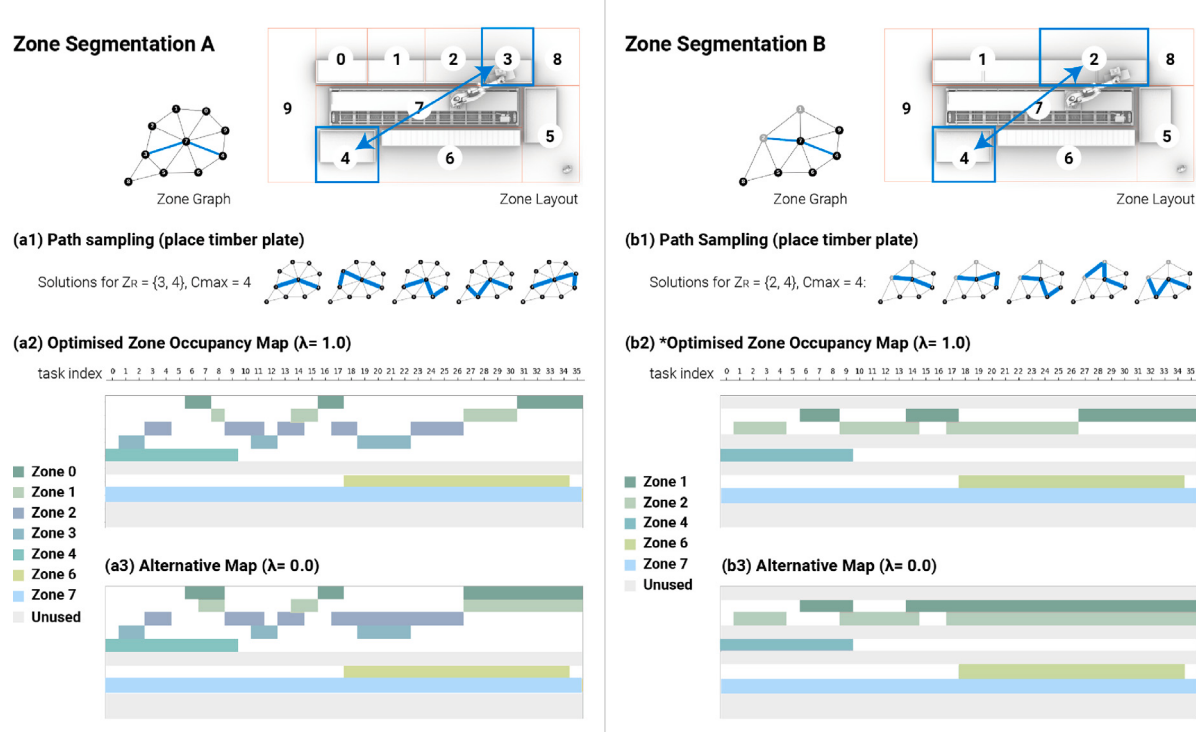


Fig. 7. Work zone generation process for two segmentation options. (a1) and (b1) show the sampled paths for a given task, e.g. pick-and-placing a timber plate. (a2) and (b2) shows the results after optimisation with $\lambda = 1.0$, resulting in a cleaner result than the alternative (a3) and (b3) where $\lambda = 0.0$. * The occupancy map in (b2) was used in the fabrication.

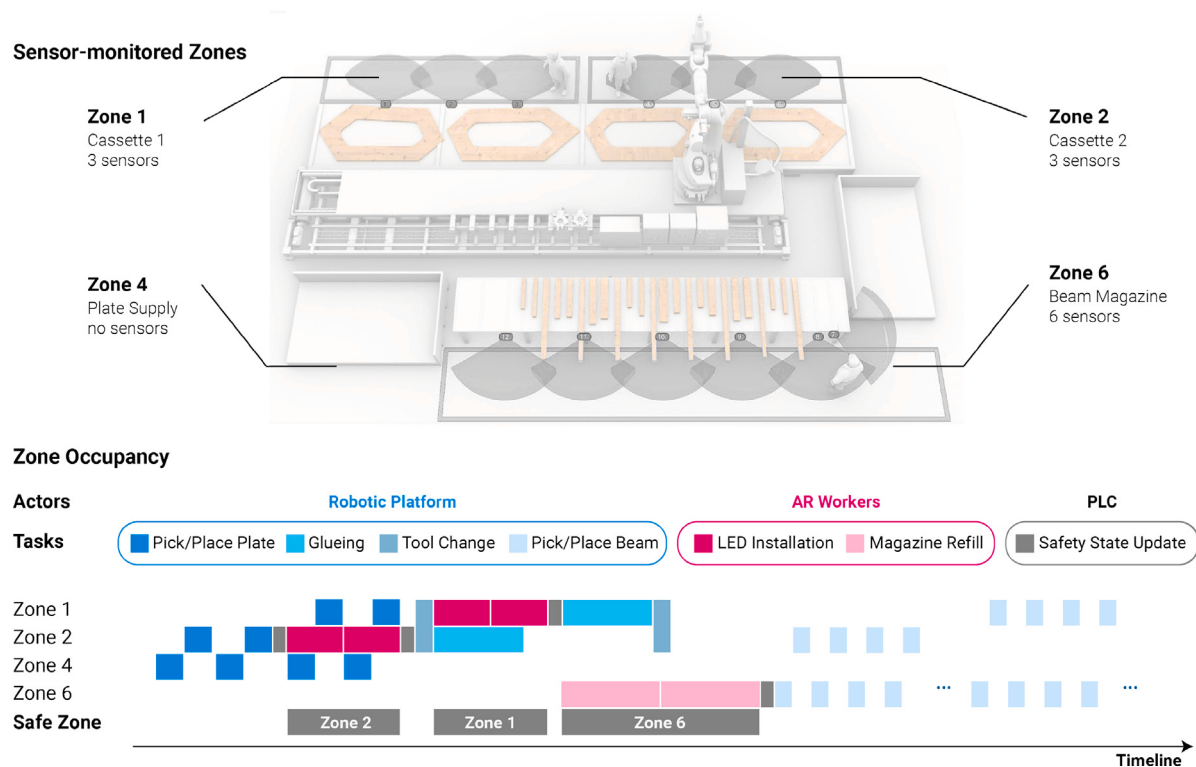


Fig. 8. Safety zone setup and HRC tasks in relation to the safety zones.



Fig. 9. Gantt chart of the HRC process simulation at different success probabilities. (a) 100% for both actors (b) Robot has 20% error likelihood (c) Human has 20% error likelihood (d) A scenario without HRC, i.e., robots are paused when humans are working. (A 20% error likelihood was chosen here referencing the threshold stated in the Pareto Principle — 20% of the causes account for 80% of the consequences [75]. This threshold can also be chosen based on individual project criteria or past performance data.)

the beam magazine, each beam is first converted to a wire frame and then combined with the label information into geometry messages. Additionally, the robotic tasks contain low-resolution meshes of the elements for AR visualisation in case a human needs to take over the operation, along with TCP values used for trajectory simulations. The information above is converted to a format compatible with the HoloLens app using the Vizor plugin [67].

5. Discrete event simulation

Simulation is a critical component of evaluation and validation due to the financial, time and human resources required to evaluate during physical fabrication at the industry partner's site. Based on the defined prefabrication tasks, we applied discrete event simulation (DES) to examine system performance metrics under various dynamic factors in the worker pool. The two performance metrics are total task completion time and percentage of robot utilisation.

Since the full prefabrication sequence also included tasks that were not relevant for HRC, e.g. milling and sawing operations that are too dangerous for humans to be in close proximity, we only used a subset of these tasks, which required human collaboration, for the simulation. For a quantitative understanding of the robotic task sequence, we refer readers to the paper [66].

5.1. Simulation setup

The process definition was first exported in a comma-separated values file containing the tasks, target actors, and an estimation of duration for each task referencing methods-time measurement estimates.

We also make the following assumptions for the simulation: (1) skill selection by each worker does not change during execution, i.e., we assume that the worker does not lose/acquire skills in the course of a production sequence; (2) if a human task fails, the re-execution takes the same amount of time, i.e., we assume that similarly skilled workers can complete tasks in a similar amount of time; (3) if a robotic task fails, the re-execution takes double the time it would a robot, i.e., we applied a constant multiplier to account for the time needed to

notice a failure, access the materials, and conduct the same task. We applied a multiplier of 2 based on our estimation from past experience, which modelled an adequately strong penalty effect when evaluating the performance time. However, given the inherent variability of how re-execution is carried out, this multiplier should ideally be dynamic and backed by empirical data, if available.

Below, we present a scenario exploration by varying several parameters in the DES and comparing it against a baseline scenario (Fig. 9a). The baseline has two human actors and one robotic actor with a 100% success rate in all actions.

5.2. Worker team composition

Given an input task distribution, the simulation can provide an estimate of the optimal worker team size to participate in the process. With an increase in team size ($|Team(\tau)|$), the duration of task completion decreases and plateaus when the team reaches a size of 3, as seen in Fig. 10 left. In other words, assigning a team larger than three would have diminishing rewards for this particular set of tasks. This plateau would likely occur with more or fewer workers in different construction scenarios. For instance, if there are more robotic resources, e.g., a dual-robot setup was used to conduct the same tasks, increasing the team size beyond three will likely continue to reduce task execution time. Vice versa, if fewer human tasks were needed for the building component, e.g., the timber cassettes required no electrical installations, the plateau may be reached at a lower team size.

Another factor is the probability of success for the worker task (P_{worker}). A lower value here can be understood as either (1) higher task difficulty or (2) lower skill/experience level of the worker with the task, both of which can result in a lower chance of success at the first attempt. A “failed” task leads to a re-allocation of the task in the worker pool if another worker is available, or the system must wait until another worker becomes free. This results in longer wait times for the robot and consequently a performance reduction. In Fig. 10 right, $P_{worker} = 80\%$ shows a 10% drop in the robot utilisation rate.



Fig. 10. Task duration and robot utilisation variations based on (a) Team size (N) (b) Worker success probability (P_{worker}) (c) Robot success probability (P_{robot}), and (d) Safety interruptions ($P_{\text{interrupt}}$).

5.3. Reaction to robotic system events

Intuitively, the robustness of robotic tasks, i.e. the probability of task success (P_{robot}), will have a high impact on the production system performance. Compared with the influence of P_{worker} , this shows a strong negative effect on the execution time and robot utilisation rate (Fig. 10 right), due partly to the proportion and speed of robotic tasks.

When humans accidentally enter a guarded safety zone, the robotic action is interrupted and needs to restart. The likelihood of such events, i.e. the probability of task interruption ($P_{\text{interrupt}}$), can also be modelled in the simulation. Given a mild safety interruption, a recovery period involves three steps: the operator must wait for the worker to exit the area, acknowledge the emergency stop error on the robot pendant, and resume the robot programme. This recovery time is estimated as a fixed duration in the simulation ($T_{\text{interrupt}} = 15$ s), after which the robot resumes the task.

More severe safety interruptions, e.g., if the worker sustained injuries or caused hardware damages, would result in longer recovery times. These rarer but more severe interruptions were outside the scope of this simulation. As shown in Fig. 10, when 80% of robotic tasks are interrupted under the described conditions, the task duration increases by less than two minutes.

5.4. Summary and limitations

Simulation tools allow designers to test different task sequences and validate design decisions, e.g., whether a team size is appropriate and identify bottlenecks in a sequence. Results of the discrete event simulation can be visualised as Gantt charts to examine the different scenarios. Fig. 9 shows the differences between the ideal baseline scenario where both humans and robot execute tasks with a 100% success rate (a), and when either actor has occasional errors (b and c). The redistribution of tasks as a response to a failed first attempt is shown in yellow.

We highlight two insights that can be gained from the simulations. First, the results validated the performance benefit of parallel HRC processes for this task sequence. Compared to a non-collaborative process where humans and robots cannot work in parallel (Fig. 9d), i.e., eliminating overlapping portions in the Gantt chart, the simulation shows around 30% reduction in task execution time with the baseline HRC scenario (Fig. 9a).

Second, we found that the probability of robotic task success has by far the largest influence on the production system performance, followed by the success probability of the workers, with task interruptions showing the least influence (Fig. 10). This indicates that, under the defined simulation condition (1 robot and 2 humans), the robot presents a bottleneck for this sequence.

It is important to note that the accuracy of the simulation depends heavily on user-defined simulation assumptions. This means the results above only provide a relative comparison but do not produce accurate performance projections. In particular, we note two limitations under these assumptions. First, we applied certain simplifications, excluding unlikely events such as severe interruptions or changes in worker skills during production. These cases are, however, important from a human factors perspective. Second, given limited real-world data during the design phase, we estimated the performance times, e.g., 2x penalty of a worker executing a robot task. This simplification of reality is a shortcoming we address further in the outlook 8.2, where data-driven approaches are suggested. Nevertheless, in the case of re-executing tasks, using a higher penalty, e.g., 3x or 4x, would not affect the conclusions of the simulation, but rather emphasise the robot bottleneck that was already evident under the 2x assumption.

6. User study

Since conducting user studies concurrent to production incurs risks for the project partners, we conducted an evaluation using AR simulations around the real robotic platforms as a proxy for the real environment (see Fig. 11). The study has two goals: (1) to attain a usability benchmark of the AR-based collaborative system, complemented by observations and qualitative feedback from carpenters, and (2) to understand user preferences and acceptance levels with regard to the three types of AR interactions (task, team, and process) during human-robot collaboration.

6.1. Participants

We aimed at a high degree of ecological validity and, as such, invited 8 workers from the industry partner to take part in the study. The participants were between 21 and 63 years old (Mean = 43, SD = 16.3). Their work experience in carpentry ranged from 3 months to 48 years; two were apprentices, and six were carpenters. None of the workers had extensive experience with AR, but three had used a HoloLens 2 before.

6.2. Materials

We compiled the AR application on four HoloLens 2 units for the study. We alternated using different pairs of devices to minimise the risk of low battery or device overheating, even though each device has a 2-3 h battery life [63]. A 20 × 20 cm marker was fixed on the metal profile in the centre of the robotic platform to localise the AR overlay. The position of the marker was pre-calibrated in the AR application before the participants put on the HoloLens.

We conducted a spatial mapping of the fabrication hall on each headset prior to running the study to ensure tracking stability. We did not experience tracking loss that disrupted the study, though we occasionally noted a slight shift (1–2 cm) in the holograms during movement over long distances. However, this effect subsided when one approached the object (regardless of its position in space). The observed deviation between the physical and virtual robot was in the range of 1–4 cm. This did not affect task execution, because all tasks were carried out in the simulated AR environment.



Fig. 11. Simulated environment for the user study at the Large Scale Construction Robotic Laboratory (LCRL) in Waiblingen. Robotic simulation (white), cassette table (grey), cassette plates (blue) and beams (green) are visualised (image through the HoloLens 2 headset).

6.3. Study design

Each study involves a single trial followed by a questionnaire and a semi-structured interview. The tasks in the trial resemble the real cassette prefabrication tasks but are adapted for completion without physical elements over a shorter duration. The physical robot remains stationary, and robotic tasks are shown using an AR simulation overlay. The tasks are carried out in one session without breaks.

Each participant wore a HoloLens and had an assisting “teammate” with whom to do the tasks. The teammate was a member of the research team who was aware of the task procedures and conducted similar tasks with the participants in tandem. All participants had the same teammate. We decided against pairing two new users in one team because the influence one user has on another introduces irrelevant complexity and confounding factors.

6.4. Measurements

In addition to demographics (age and work experience in timber construction), we collected three measurements from each participant: (1) task duration, (2) System Usability Scale (SUS), and (3) results of the semi-structured interviews. The SUS questionnaire was translated into German from Brooke’s 10-item SUS scale [76]. The semi-structured interview included four topics:

AR-supported Task Sharing: What is your overall experience and impression about this process?

Task Interactions: How did you find the task interface? What was challenging for you?

Team Interactions: How did you find the process of requesting help/rejecting a task? What was challenging for you?

Process Interactions: How did you find the process of overtaking a failed robot task? What was challenging for you?

6.5. Task design

To gather user feedback on the interactive features in the AR system, we created opportunities for these interactions by pre-programming “errors” during task completion. Each user performed the following tasks (marked T1–T9): Pick two wires with correct markings out of four and place them on the cassette in AR (T1). Move to the second cassette zone (T2). Pick and place another set of wires, but the markings are intentionally incorrect; the user can either reject the task or request help from their teammate (T3). Move to the magazine zone (T4). Pick two beams out of four that are correct in length and place them on the magazine in AR (T5). Pick and place another set of beams, but one input beam is missing; the user can again either request help or reject the task (T6). Move to the monitoring zone and oversee robotic pick and place procedures (T7). One procedure “fails”, requesting the user to overtake the execution (T8). The same overtake task is repeated (T9). Dynamic task allocation was used during T3, T6 (from the worker to their partner) and T8, T9 (from robot to the worker).

While T1 and T5 familiarise the user with task interactions in AR, T3 and T6 expose the user to the team interaction features with intentional errors. After the monitoring task (T7), T8 and T9 simulate an automation failure event and require the user to interact with the task list by overtaking a failed robotic task. T2, T4, and T7 are shared sequential tasks where the “teammate” (research assistant) and the participant need to both acknowledge completion of each task, while all other tasks are sent in parallel to both users for independent execution (see Fig. 13).

6.6. System performance

During the study, we observed a response time of around one second on the AR devices (from the moment of a button press to receiving new task visualisations). To understand this in more detail, we performed a post-hoc performance analysis replicating the study conditions. The same PC (2.6 GHz CPU, 32 GB of RAM), HoloLens 2 device, and wireless network configuration (5 GHz router, with only the PC and HoloLens connected to the network) were used.

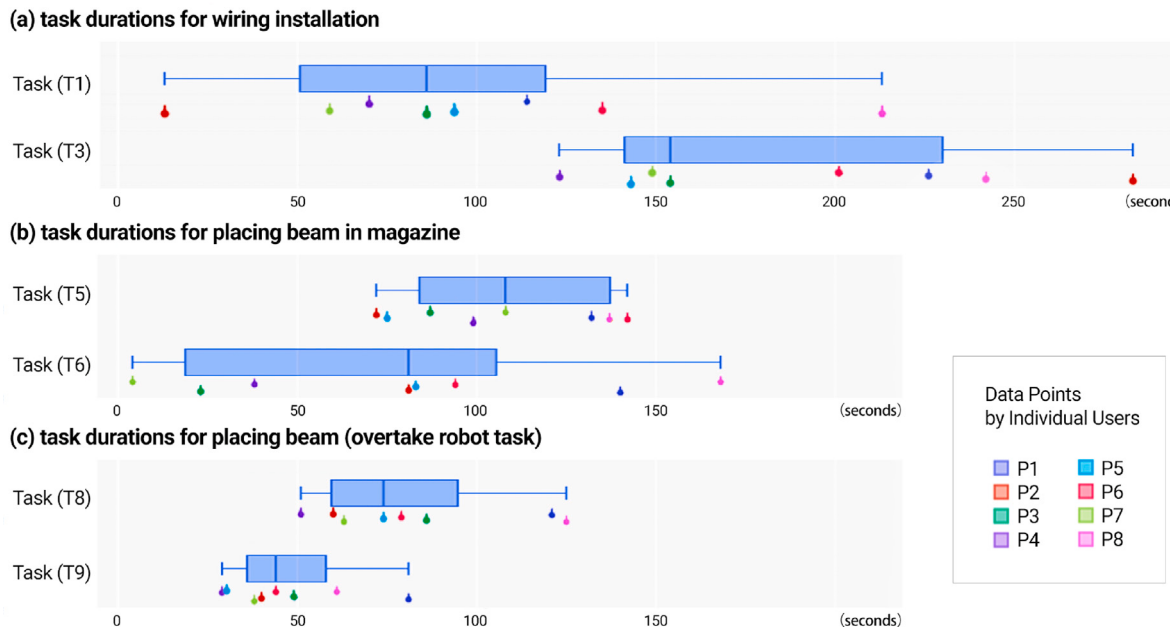


Fig. 12. Task durations for main tasks in the user study. (a) Manual installation of electrical wires: T1 under normal execution, T3 under intentional error condition. In T3, all users used the *help* function. (b) Manual placement of beams in the magazine: T5 under normal execution, T6 under intentional error condition. In T6, 4 users *rejected* the task, 5 users requested *help*. (c) Human overtaking failed robotic tasks: T8 first-time execution, T9 executing for a second time.

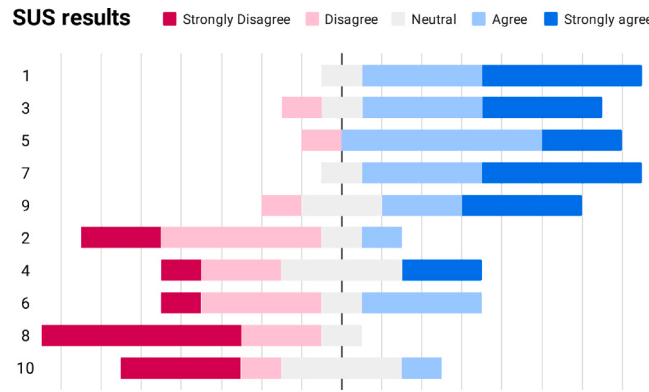


Fig. 13. System Usability Scale (SUS) results of the AR user study ($N = 8$). The numbers on the left correspond to question numbers in the SUS questionnaire; the top five questions are agreements, and the bottom five are disagreements [76].

The time required for performing dynamic allocation, from detecting a task in the queue to deciding on the worker team, averaged $\bar{A}_{alloc} = 42$ ms. From the task completion event, i.e., button press on the HoloLens, to receiving the task visualisation, i.e., objects were shown on the HoloLens, the average total response time was $\bar{A}_{total} = 792$ ms. Because the study included two humans executing in parallel, this total duration also included the processing time of a parallel task for the human partner $\bar{A}_{parallel} = 100$ ms. The average time for sending visualisation only, e.g., for robotic tasks and tasks completed by another worker, was $\bar{A}_{dispatch} = 6$ ms. **Table 3** presents a complete list of recorded response times.

The HoloLens application remained at 59–60 fps during use. The maximum CPU time per frame observed was 17.9 ms. The peak memory use was 774.7 MB out of 2048 MB available (38%).

6.7. Study results

The SUS score of the AR system has a mean of 72.7 and a standard deviation of 12.7. Pearson's correlation coefficient between the

Table 3

Response time of system components. (In this setup, the worker pool contained two workers executing tasks in parallel.)

Response time	μ (ms)	σ (ms)
Pool computation	450	165
Parallel task process	100	42
Network (Roundtrip)	68	31
Allocation decision	42	30
Task server response	35	21
Dispatch visualisation	6	4
Total	792	31

participant's age and SUS rating showed a strong negative relationship $r = -0.68$, that is, the older a participant, the more negative the SUS score.

The overall SUS ratings were similar to those of an existing exploratory user study ($N = 16$, age 25–35) employing a similar system without team and process interaction features (Mean = 73.5, SD = 12.2) [65]. Similar to this previous study, the item that performed worst was question 4: “I think I would need the support of a technical person to be able to use this”. Between a score of 1–5 (5 being the worst), the mean score for this question was 3.0 with a standard deviation of 1.41.

The task durations for the key human tasks are summarised in **Fig. 12**. Between the tasks without error (T1 and T5) and those with intentional errors (T3 and T6), the latter took roughly 50% longer for users who requested help of the partner to complete. Three users in T6 rejected the task, resulting in a much shorter task duration, as logged by the system. When overtaking the robotic task, the second execution (T9) showed a clear improvement in task speeds from T8, likely due to the learning effects.

6.8. Qualitative feedback

At the end of the study, we conducted a 15-min interview with the participants. The transcriptions are translated from German to English and summarised below. The results are grouped into the following four categories:

AR-supported Task Sharing: 5/8 used the HoloLens for the first time, and the system “*took some getting used to, but once you get it, it is very easy*”. Most users found the visualisation easy to understand. One user who was a carpentry machine operator saw this as a “*change in the profession of machine operators*” and with the robot “*silly repetitive tasks don't have to be always done by hand*”.

Team Interactions: Most participants chose to use “Help” instead of “Reject” for the problematic tasks and made similar comments that they would not use the reject function in reality because it would lead to problems for the task and would be inappropriate in a professional setting. Most would prefer either to ask for help or to have an option to set aside the task temporarily. All users found the help function useful and noted that this meant they did not have to leave their workspace to ask for help and that it was more practical when the partner is far away and calling out by voice in a loud hall is not desirable.

Task Interactions: The task instructions were found to be simple and straightforward, but the simulated nature of the manual tasks made some users feel it “*was like a videogame*”. The most prominent usability issue is the limited field of view on the HoloLens 2 which led to users needing to “*look around a lot for the elements*”. One user also commented that once one knows the task process, the descriptions will no longer be needed, but it is useful when one starts a new process.

Process Interactions: During the robotic monitoring task, the task list provided an overview of the process. Some commented that during manual task execution, this task list was useless, which matched our design assumptions. Most users found the process of overtaking a robotic task to be easy, but several found it very boring to stand next to the robot just “*doing nothing and observing*” during the monitoring process. Since the robot did not make physical motions, we did not evaluate workers’ perception of safety when overtaking these robotic tasks. However, one participant hinted at the impact of working in pairs on safety perception – “*I generally think that when you work with robots, you have to be in pairs because one always has an eye on the other one ... I can be alone only when the robot is not moving*”.

7. Fabrication demonstrator

Finally, we summarise the physical execution process implemented during three batches of timber cassettes for the livMatS Biomimetic Shell and present the feedback from workers participating in the project. Using the multi-user HRC system, two humans and one robot worked in collaboration to complete the assembly of timber cassettes.

7.1. Robotic execution

Four different end-effectors were used for the robotic fabrication steps, and the tool change was managed through the fabrication control system — each task was linked with the respective tool number, which ensured the correct tool selection and execution of the corresponding KRL subroutines. The implementation of safety frames at each bay ensured accurate end-effector orientation, while the pre-simulation of the manufacturing process using Virtual Robots (see 4.6) enhanced workflow reliability and efficiency by identifying potential fabrication errors prior to physical production. Encapsulation of related information into executable tasks enabled mostly error-free execution of the machine code throughout the manufacturing process.

During the three batches where AR was integrated, the robotic execution did not encounter errors. Throughout the entire 6-week fabrication process, robotic errors that occurred were primarily hardware-related or due to material heterogeneity. Specifically, when nailing wooden nails, which were used for temporary fixation of the components during the assembly process, there were occasional nail breakages if a knot was present at the nail position. These nail breakages sometimes led to a blockage in the nail gun and required humans to resolve the hardware issue and re-insert the wood nails. During these instances, the operators stopped the robot and resolved the issues manually with hand tools.

7.2. AR-supported human–robot collaboration

Two HoloLens 2 units were used in the demonstration and were connected via WiFi to the worker pool. The worker pool connected via the same WiFi to the fabrication server running on a different PC. The AR view from the HoloLens is illustrated in Fig. 2. In addition to coordinating the collaboration, the interface supported two manual tasks in AR, which were executed using paper documentation in all other production batches.

First, the light installation required a worker to install two linear rails on the cassettes, affix the LED strips to each rail, and connect the two in the centre. Two workers were connected to the system at one time and worked respectively on two different cassettes in the same work zone. A comparison of the execution of this task with paper documentation v.s. AR is shown in Fig. 14(a, b).

The second task is refilling the material storage at the back of the robotic platform. Due to the need to control the wood moisture content before placing and glueing, the wood was taken out of the moisture-control chamber and loaded into the beam magazine shortly before they were placed. In addition to preparation outside of the main working area, this task involved the identification of a beam by a sticker on the material and placing it in the correct slot of the material supply station as indicated in Fig. 14(c, d).

To understand the ergonomics of this process, we highlight the implications of the AR headset’s field of view (FOV) during these two tasks. The HoloLens 2 provides a horizontal FOV of 43 degrees and a vertical FOV of 29 degrees [77]. Since the light installation task required the user to affix the strips manually, the user mostly remained at arm’s length from the object. At an average length of 75 cm, the AR projection would cover 0.95 m diagonally (0.6 m horizontal, 0.4 m vertical). Since the LED strips ranged from 0.85 m to 2.1 m (average length 1.625 m), this meant that the users almost always had to rotate their head to capture the entire object.

During the magazine refill task, the beams ranged from 0.5 m to 2.2 m (average length 1.09 m). The beam magazine bay was 1.3 m deep, so when placing the beam, the user stood roughly 1.5 m away from the inside edge of the refill station. This provided a 1.9 m projection coverage diagonally (1.2 m horizontal, 0.8 m vertical). For most beams, the AR visualisation can cover the entire object.

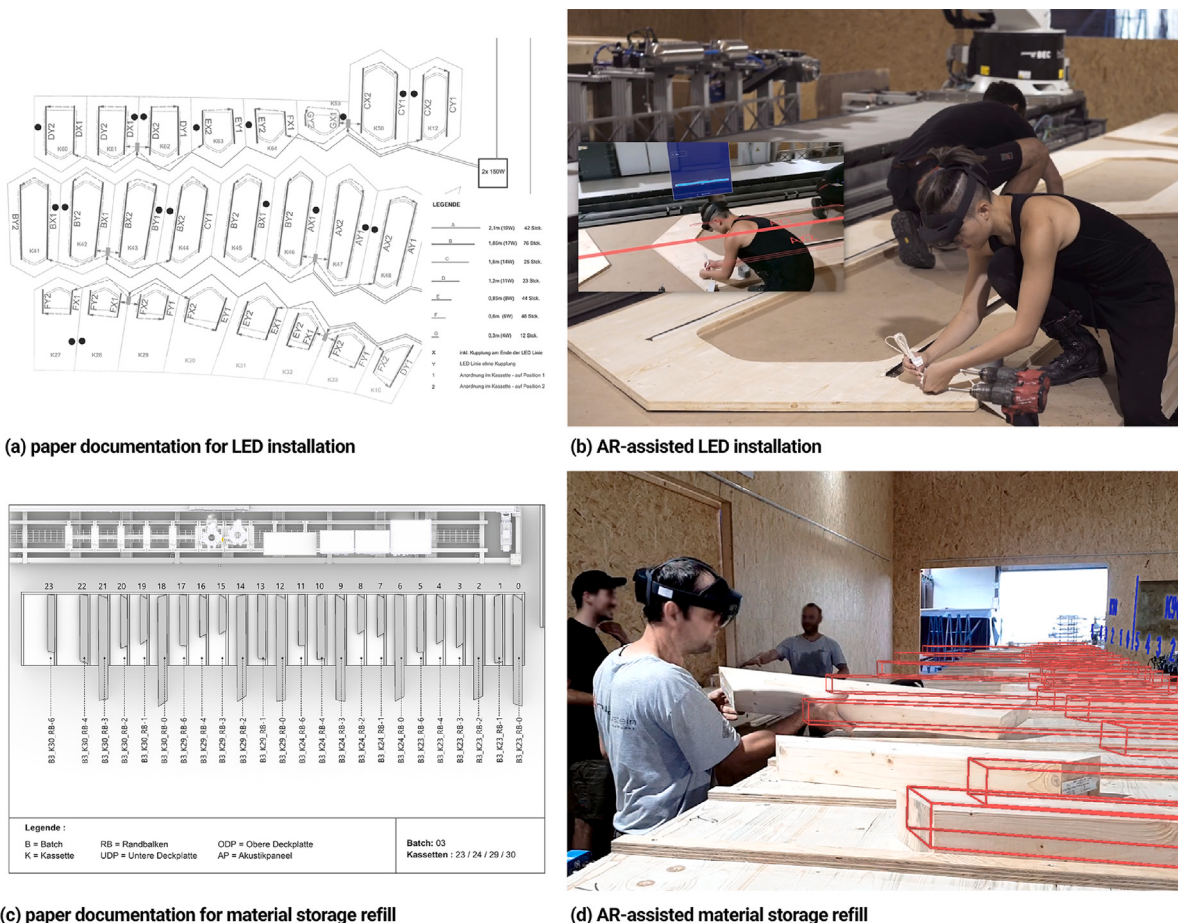
7.3. Results and feedback

The fabrication demonstration was conducted during three batches of cassette prefabrication over one day. The system enabled two humans equipped with HoloLens 2 headsets to work alongside the industrial robot. The worker pool dynamically allocated tasks among the two workers, allowing them to work in parallel with each other on two different cassettes.

The headsets displayed corresponding task instructions, safety zone information, and robot visualisations during each task. Similar to the user study 6.2, we did not experience battery issues or tracking loss during production and observed a similar response time and accuracy of the overlay. Positional deviations between the real and virtual objects fell in the 1–4 cm range, which was noticeable during the manual tasks but did not affect overall task execution.

The workers participating in the prefabrication process found the AR application most useful for two tasks. First, the magazine refill task originally required back-and-forth references to a stack of paper documentation to identify the correct beam and place it in the correct location and orientation. Because some beam geometries were very similar, they required multiple rounds of checking by two workers. The in-situ AR display allowed a much more efficient alternative.

Second, since the prefabrication area was protected from the rest of the hall with a temporary enclosure, there was no visibility of the robotic process unless the worker physically entered the workspace. The AR simulations of the robotic tasks allowed users to visualise the



between sessions to mitigate low battery or overheating issues. In real-world applications where the systems need to be used continuously without breaks, the current capacity of the headsets can present a challenge. However, we remain optimistic given the rapid evolution and improvements in new AR headsets.

For simplicity, the simulations of the HRC process used an event-based solver instead of time-based simulations. The DES approach is less time-consuming and allows rapid feedback during process design, but the latter is more appropriate for capturing more detailed dynamics. Incorporating time-based simulation can enhance the temporal resolution of the results and provide more granular insights on human–robot interaction dynamics. Furthermore, digital human modelling tools can be included to emulate human behaviours to greater detail [80]. The current simulation results are also heavily dependent on assumptions for task durations, for which data-driven predictive approaches should be used to inform these assumptions [66].

During execution, the dynamic task allocation by the worker pool was a critical function that enabled the system to coordinate multiple users and facilitate process interactions. However, the current allocation process mainly serves as a “failsafe” for unexpected situations, where human workers receive the re-allocated task. Dynamic reassessments to robots would be important for more advanced human–robot teaming, though they may be more difficult or risky to test in production environments. Additionally, if not enough workers, or appropriately skilled workers, are available in the pool, the system will not be able to progress. Since being able to test the system during live production was a precious opportunity, we did not allow this to occur. If the system was used over a longer period, such events, whether due to technical issues or human factors, may become a source of failure and need to be mitigated. Additional functions can be incorporated here to raise alerts when detecting these issues, e.g., worker fatigue, unexpected errors, or inactivity, and automatically modify the configuration.

In the current safety zone generation process, each workstation was large, and the layout was rather constrained; the segmentation problem was therefore fairly trivial. For larger search spaces, the segmentation algorithm would need to be improved to generate good solutions. For crowded environments with many possible collisions, computing path feasibility may also take a long time, which we avoided by having relatively sparsely populated work areas and a short task sequence.

A critical aspect of industrial human–robot collaboration is the safety certification and declaration of conformity that the distributor of the machines and systems must carry out and provide each time the system is reconfigured or adapted. According to IEC 62061 and ISO 13849 [81,82], risk and hazard analysis are required for the entire system and its processes, and appropriate measures to be taken to protect against hazards need to be identified. The implementation of this currently manual certification process requires expert knowledge and is very time-consuming. This is especially true for the use case described above, where reconfigurable, transportable robotic systems are used to prefabricate timber components at different locations, as the process must be repeated for each reconfiguration. In this respect, the prospect of semi-automated certification procedures supported by software, e.g. in simulation environments, is promising in order to reduce the effort in the described application and thus enable such systems.

In addition to external safety systems, workers’ perception of safety and trust in the robotic system are equally important for the successful deployment of human–robot collaboration in the workplace. Our user study focused on evaluating the AR interface, but did not focus on capturing safety perception in the measurements. Recent studies have shown that a separation of work areas increases workers’ perceived safety by promoting trust and team identification [28]. Systems that can enhance the perception of trust and safety should be investigated in future work.

8.2. Outlook

Designing for human–robot collaboration for timber prefabrication needs to account for system, human, and design-oriented factors [11]. The implementation above focused mainly on the first two. Whether the results can be extrapolated to applications in other design variants, e.g., using more dexterous joining techniques [83], or dealing with more dynamic material behaviours [54], where the length and proportion of human and robotic tasks will likely be very different, is left to future work.

The HRC simulation process will greatly benefit from data-driven approaches for estimations of both human and robot task durations [84]. Machine learning methods for lead time predictions are widely explored in the manufacturing literature [85] and would be an important next step to enhance the simulation quality and inform better HRC designs. It is important to note that such automated predictions should remain transparent, steerable, and understandable to the users, thus empowering them to design based on real-world data rather than fully automating the design process. Evaluating an HRC system in a real production setting is both risky and resource-intensive, but it also provides better ecological validity of the results. With the increasing proliferation and standardisation of HRC, we expect that there will be more opportunities for such field studies “in the wild” [86].

More advanced safety features using human sensing and intent prediction can also be incorporated to support more intelligent adaptations during HRC [87,88]. This would open the possibility to extend the safety zone visualisation beyond statically defined information to more dynamic and predictive information to enhance collaboration fluency. However, such intelligent systems should always allow humans to understand the decisions transparently and remain in control. Facilitating user control keeps humans effectively in the loop to ensure smooth collaboration [89] and has important implications on the perception of agency and psychological needs [90,91]. With the increase in adoption of automation in construction industries, safe, transparent, and flexible systems that effectively facilitate closer collaboration of human and robotic actors are highly important for the well-being of the workers and the productivity of the industry.

9. Conclusion

This research presents a cohesive HRC implementation for large-scale building prefabrication, integrating interdisciplinary knowledge from contributors in architecture, computational design, visualisation, manufacturing, and human–robot interaction disciplines. Given the multitude of information in digital construction processes and a large body of existing work on AR implementations for HRC [45], our design efforts contribute (1) a systematic organisation of AR interface elements based on the level of automation (LoA) in construction tasks and (2) an empirical evaluation with construction workers on various task and process interaction possibilities. Moving beyond single-user, homogeneous collaboration setups, the AR system is driven by a worker pool that enables multi-user coordination under dynamic production conditions. Building on a skill-based approach for HRC in timber construction [11], the worker pool formalises the task allocation process and facilitates adaptation to unexpected events by the multi-human–robot team, e.g., requesting help from/delegating tasks to one another. A zone-based safety workflow enables human collaboration with heavy-payload industrial robots that do not have advanced safety features. Using sensor-monitored zones to regulate the shared space between humans and robots over time, the proposed method optimises spatial constraints during computational design and planning, ensuring that safety is addressed early on. Combining a physical demonstration, digital simulations, and a user study, the results of our mixed-methods evaluation contribute empirical and practical insights on various facets of adopting the HRC workflow. Lastly, by outlining current limitations and outlook for improvements, we hope to inform future research efforts towards more flexible, fluent, and safer human–robot collaboration workflows for prefabrication and construction.

CRediT authorship contribution statement

Xiliu Yang: Writing – review & editing, Writing – original draft, Visualization, Software, Project administration, Methodology, Investigation, Formal analysis, Data curation, Conceptualization. **Felix Amtsberg:** Writing – review & editing, Supervision, Project administration, Methodology, Investigation, Funding acquisition, Conceptualization. **Benjamin Kaiser:** Writing – review & editing, Software, Methodology, Conceptualization. **Lior Skoury:** Writing – review & editing, Investigation, Conceptualization. **Tim Stark:** Writing – review & editing, Investigation. **Simon Tremel:** Writing – review & editing, Investigation. **Nils Opgenorth:** Writing – review & editing, Investigation. **Aimée Sousa Calepso:** Writing – review & editing, Investigation. **Michael Sedlmair:** Writing – review & editing, Supervision, Resources. **Thomas Wortmann:** Writing – review & editing, Supervision, Resources. **Alexander Verl:** Writing – review & editing, Supervision, Resources. **Achim Menges:** Writing – review & editing, Supervision, Resources, Funding acquisition.

Declaration of competing interest

The authors declare that they have no known competing financial interests or personal relationships that could have appeared to influence the work reported in this paper.

Acknowledgements

This research was supported by the Deutsche Forschungsgemeinschaft (DFG; German Research Foundation) under Germany's Excellence Strategy – EXC 2120/1 – 390831618 and BBSR as Zukunft Bau Project "MRK II Projektnr. 10.08.18.7-22.22". We would like to thank the student assistant Clara Blum as well as the industry partners müllerblaustein HolzBauWerke and BEC Robotics for their support.

Data availability

Data will be made available on request.

References

- [1] J.M. Davila Delgado, L. Oyedele, A. Ajayi, L. Akanbi, O. Akinade, M. Bilal, H. Owolabi, Robotics and automated systems in construction: Understanding industry-specific challenges for adoption, *J. Build. Eng.* 26 (2019) 100868, <http://dx.doi.org/10.1016/j.jobe.2019.100868>.
- [2] H.J. Wagner, M. Alvarez, A. Groenewolt, A. Menges, Towards digital automation flexibility in large-scale timber construction: integrative robotic prefabrication and co-design of the BUGA wood pavilion, *Constr. Robot.* 4 (3–4) (2020) 187–204, <http://dx.doi.org/10.1007/s41693-020-00038-5>.
- [3] S. Parascho, Construction robotics: From automation to collaboration, *Annu. Rev. Control. Robot. Auton. Syst.* 6 (Volume 6, 2023) (2023) 183–204, <http://dx.doi.org/10.1146/annurev-control-080122-090049>.
- [4] Y. Fu, J. Chen, W. Lu, Human-robot collaboration for modular construction manufacturing: Review of academic research, *Autom. Constr.* 158 (2024) 105196, <http://dx.doi.org/10.1016/j.autcon.2023.105196>.
- [5] Edvard, P.G. Bruun, Ian Ting, S. Adriaenssens, S. Parascho, Human–robot collaboration: a fabrication framework for the sequential design and construction of unplanned spatial structures, *Digit. Creat.* 31 (4) (2020) 320–336, <http://dx.doi.org/10.1080/14626268.2020.1845214>.
- [6] D. Mitterberger, S.E. Jenny, L. Vasey, E. Lloret-Fritschi, P. Aeijmelaes-Lindström, F. Gramazio, M. Kohler, Interactive robotic plastering: Augmented interactive design and fabrication for on-site robotic plastering, in: Proceedings of the 2022 Conference on Human Factors in Computing Systems, CHI, no. 174, Association for Computing Machinery (ACM), 2022, pp. 1–18, <http://dx.doi.org/10.1145/3491102.3501842>.
- [7] L. Atanasova, D. Mitterberger, T. Sandy, F. Gramazio, M. Kohler, K. Dorfler, Prototype as artefact - design tool for open-ended collaborative assembly processes, in: Proceedings of the 40th Annual Conference of the Association for Computer Aided Design in Architecture: Distributed Proximities, ACADIA, Vol. 1, 2020, pp. 350—359, URL https://papers.cumincad.org/data/works/att/acadia20_350.pdf. (Accessed 18 December 2024).
- [8] F. Amtsberg, X. Yang, L. Skouri, H.J. Wagner, A. Menges, iHRC: An AR-Based Interface for Intuitive, Interactive and Coordinated Task Sharing Between Humans and Robots in Building Construction, in: Proceedings of the 38th International Symposium on Automation and Robotics in Construction, ISARC, 2021, pp. 25–32, <http://dx.doi.org/10.22260/ISARC2021/0006>.
- [9] B. Lee, M. Sedlmair, D. Schmalstieg, Design patterns for situated visualization in augmented reality, *IEEE Trans. Vis. Comput. Graphics* (2023) 1–12, <http://dx.doi.org/10.1109/tvcg.2023.3327398>.
- [10] P. Fleck, A.S. Calepso, S. Hubenschmid, M. Sedlmair, D. Schmalstieg, RagRug: A toolkit for situated analytics, *IEEE Trans. Vis. Comput. Graphics* 29 (7) (2023) 3281–3297, <http://dx.doi.org/10.1109/tvcg.2022.3157058>.
- [11] X. Yang, F. Amtsberg, M. Sedlmair, A. Menges, Challenges and potential for human–robot collaboration in timber prefabrication, *Autom. Constr.* 160 (2024) 105333, <http://dx.doi.org/10.1016/j.autcon.2024.105333>.
- [12] N. Opgenorth, T. Cheng, A.P.R. Lauer, L. Skouri, E.S. Sahin, T. Stark, Y. Tahouni, S. Tremel, M. Göbel, L. Kiesewetter, C. Schlopschnat, M.B. Zorn, X. Yang, F. Amtsberg, H.J. Wagner, D. Wood, O. Sawodny, T. Wortmann, A. Menges, Multi-scalar computational fabrication and construction of bio-based building envelopes: The LivMatS biomimetic shell, in: FABRICATE 2024, UCL Press, 2024, pp. 22–31, <http://dx.doi.org/10.2307/ji.11374766.7>.
- [13] P. Ruttico, M. Pacini, C. Beltracchi, BRIX: an autonomous system for brick wall construction, *Constr. Robot.* 8 (2) (2024) <http://dx.doi.org/10.1007/s41693-024-00123-z>.
- [14] Z. Bi, C. Luo, Z. Miao, B. Zhang, W. Zhang, L. Wang, Safety assurance mechanisms of collaborative robotic systems in manufacturing, *Robot. Comput.-Integr. Manuf.* 67 (2021) 102022, <http://dx.doi.org/10.1016/j.rcim.2020.102022>.
- [15] C. Vogel, N. Elkmann, Novel safety concept for safeguarding and supporting humans in human-robot shared workplaces with high-payload robots in industrial applications, in: Proceedings of the Companion of the 2017 ACM/IEEE International Conference on Human-Robot Interaction, HRI '17, ACM, 2017, pp. 315–316, <http://dx.doi.org/10.1145/3029798.3038314>.
- [16] M. Bdiwi, I. Al Naser, J. Halim, S. Ihlenfeldt, Towards safety4.0: A novel approach for flexible human-robot-interaction based on safety-related dynamic finite-state machine with multilayer operation modes, *Front. Robot. AI* 9 (2022) <http://dx.doi.org/10.3389/frobt.2022.1002226>.
- [17] M.J. Rosenstrauch, J. Kruger, Safe human-robot-collaboration-introduction and experiment using ISO/TS 15066, in: 2017 3rd International Conference on Control, Automation and Robotics, ICCAR, IEEE, 2017, pp. 740–744, <http://dx.doi.org/10.1109/iccar.2017.7942795>.
- [18] J. Arents, V. Abolins, J. Judvaitis, O. Vismanis, A. Oraby, K. Ozols, Human–robot collaboration trends and safety aspects: A systematic review, *J. Sens. Actuator Netw.* 10 (3) (2021) <http://dx.doi.org/10.3390/jstan10030048>.
- [19] Robots and Robotiq Devices — Collaborative Robots, Standard, International Organization for Standardization, Geneva, CH, 2016, URL <https://www.iso.org/standard/62996.html>. (Accessed 24 July 2024).
- [20] P. Karagiannis, N. Kousi, G. Michalos, K. Dimoulas, K. Mparis, D. Dimosthenopoulos, Ö. Tokçalar, T. Guasch, G.P. Gerio, S. Makris, Adaptive speed and separation monitoring based on switching of safety zones for effective human robot collaboration, *Robot. Comput.-Integr. Manuf.* 77 (2022) 102361, <http://dx.doi.org/10.1016/j.rcim.2022.102361>.
- [21] P.A. Lasota, G.F. Rossano, J.A. Shah, Toward safe close-proximity human–robot interaction with standard industrial robots, in: 2014 IEEE International Conference on Automation Science and Engineering, CASE, 2014, pp. 339–344, <http://dx.doi.org/10.1109/CoASE.2014.6899348>.
- [22] A. Rashid, K. Peesapati, M. Bdiwi, S. Krusche, W. Hardt, M. Putz, Local and global sensors for collision avoidance, in: 2020 IEEE International Conference on Multisensor Fusion and Integration for Intelligent Systems, MFI, 2020, pp. 354–359, <http://dx.doi.org/10.1109/MFI49285.2020.9235223>.
- [23] A.C. Simões, A. Pinto, J. Santos, S. Pinheiro, D. Romero, Designing human–robot collaboration (HRC) workspaces in industrial settings: A systematic literature review, *J. Manuf. Syst.* 62 (2022) 28–43, <http://dx.doi.org/10.1016/j.jmsy.2021.11.007>.
- [24] L. Gualtieri, E. Rauch, R. Vidoni, D.T. Matt, Safety, ergonomics and efficiency in human–robot collaborative assembly: Design guidelines and requirements, *Procedia CIRP* 91 (2020) 367–372, <http://dx.doi.org/10.1016/j.procir.2020.02.188>, Enhancing design through the 4th Industrial Revolution Thinking.
- [25] M. Bdiwi, M. Pfeifer, A. Sterzing, A new strategy for ensuring human safety during various levels of interaction with industrial robots, *CIRP Ann* 66 (1) (2017) 453–456, <http://dx.doi.org/10.1016/j.cirp.2017.04.009>.
- [26] H.J. Wagner, M. Alvarez, O. Kyjanek, Z. Bhiri, M. Buck, A. Menges, Flexible and transportable robotic timber construction platform – TIM, *Autom. Constr.* 120 (2020) 103400, <http://dx.doi.org/10.1016/j.autcon.2020.103400>.
- [27] B. M. Tehrani, A. Alwisy, Enhancing safety in human–robot collaboration through immersive technology: a framework for panel framing task in industrialized construction, *Constr. Robot.* 7 (2) (2023) 141–157, <http://dx.doi.org/10.1007/s41693-023-00101-x>.
- [28] S. You, J.-H. Kim, S. Lee, V. Kamat, L.P. Robert, Enhancing perceived safety in human–robot collaborative construction using immersive virtual environments, *Autom. Constr.* 96 (2018) 161–170, <http://dx.doi.org/10.1016/j.autcon.2018.09.008>.

- [29] C. Petzoldt, M. Harms, M. Freitag, Review of task allocation for human-robot collaboration in assembly, *Int. J. Comput. Integr. Manuf.* 36 (11) (2023) 1675–1715, <http://dx.doi.org/10.1080/0951192x.2023.2204467>.
- [30] F. Ranz, V. Hummel, W. Sihl, Capability-based task allocation in human-robot collaboration, *Procedia Manuf.* 9 (2017) 182–189, <http://dx.doi.org/10.1016/j.promfg.2017.04.011>, 7th Conference on Learning Factories, CLF 2017.
- [31] A.A. Malik, A. Bilberg, Complexity-based task allocation in human-robot collaborative assembly, *Ind. Robot.: Int. J. Robot. Res. Appl.* 46 (4) (2019) 471–480, <http://dx.doi.org/10.1108/ir-11-2018-0231>.
- [32] P.M. Fitts, Human Engineering for an Effective Air-Navigation and Traffic-Control System, Tech. Rep., National Research Council, 1951, URL <https://apps.dtic.mil/sti/pdfs/AD815893.pdf>. (Accessed 24 July 2024).
- [33] R. Müller, M. Vette, O. Mailahn, Process-oriented task assignment for assembly processes with human-robot interaction, *Procedia CIRP* 44 (2016) 210–215, <http://dx.doi.org/10.1016/j.procir.2016.02.080>, 6th CIRP Conference on Assembly Technologies and Systems (CATS).
- [34] G. Bruno, D. Antonelli, Dynamic task classification and assignment for the management of human-robot collaborative teams in workcells, *Int. J. Adv. Manuf. Technol.* 98 (9–12) (2018) 2415–2427, <http://dx.doi.org/10.1007/s00170-018-2400-4>.
- [35] P. Tsarouchi, G. Michalos, S. Makris, T. Athanasatos, K. Dimoulas, G. Chrysosolouris, On a human-robot workplace design and task allocation system, *Int. J. Comput. Integr. Manuf.* 30 (12) (2017) 1272–1279, <http://dx.doi.org/10.1080/0951192X.2017.1307524>.
- [36] M. Cramer, K. Kellens, E. Demeester, Probabilistic decision model for adaptive task planning in human-robot collaborative assembly based on designer and operator intents, *IEEE Robot. Autom. Lett.* 6 (4) (2021) 7325–7332, <http://dx.doi.org/10.1109/LRA.2021.309513>.
- [37] C. Messeri, A. Bicchi, A.M. Zanchettin, P. Rocco, A dynamic task allocation strategy to mitigate the human physical fatigue in collaborative robotics, *IEEE Robot. Autom. Lett.* 7 (2) (2022) 2178–2185, <http://dx.doi.org/10.1109/lra.2022.3143520>.
- [38] D. Antonelli, G. Bruno, Dynamic distribution of assembly tasks in a collaborative workcell of humans and robots, *FME Trans.* 47 (4) (2019) 723–730, <http://dx.doi.org/10.5937/fmet1904723a>.
- [39] D. Trentesaux, P. Millot, A human-centred design to break the myth of the “magic human” in intelligent manufacturing systems, in: *Service Orientation in Holonic and Multi-Agent Manufacturing*, Springer International Publishing, 2016, pp. 103–113, http://dx.doi.org/10.1007/978-3-319-30337-6_10.
- [40] N. Katiraei, D. Battini, O. Battai, M. Calzavara, Human diversity factors in production system modelling and design: state of the art and future researches, *IFAC- Pap.* 52 (13) (2019) 2544–2549, <http://dx.doi.org/10.1016/j.ifacol.2019.11.589>.
- [41] C. Zhang, Z. Wang, G. Zhou, F. Chang, D. Ma, Y. Jing, W. Cheng, K. Ding, D. Zhao, Towards new-generation human-centric smart manufacturing in industry 5.0: A systematic review, *Adv. Eng. Inform.* 57 (2023) 102121, <http://dx.doi.org/10.1016/j.aei.2023.102121>.
- [42] I. Gräßler, D. Roesmann, C. Cappello, E. Steffen, Skill-based worker assignment in a manual assembly line, *Procedia CIRP* 100 (2021) 433–438, <http://dx.doi.org/10.1016/j.procir.2021.05.100>.
- [43] D. Strang, N. Galaske, R. Anderl, Dynamic, adaptive worker allocation for the integration of human factors in cyber-physical production systems, in: *Advances in Intelligent Systems and Computing*, Springer International Publishing, 2016, pp. 517–529, http://dx.doi.org/10.1007/978-3-319-41697-7_45.
- [44] R. Liu, M. Natarajan, M.C. Gombolay, Coordinating human-robot teams with dynamic and stochastic task proficiencies, *ACM Trans. Hum.- Robot. Interact.* 11 (1) (2021) 1–42, <http://dx.doi.org/10.1145/3477391>.
- [45] R. Suzuki, A. Karim, T. Xia, H. Hedayati, N. Marquardt, Augmented reality and robotics: A survey and taxonomy for AR-enhanced human-robot interaction and robotic interfaces, in: *CHI Conference on Human Factors in Computing Systems, CHI '22, ACM*, 2022, <http://dx.doi.org/10.1145/3491102.3517719>.
- [46] K. Lotsaris, C. Gkournelos, N. Fousekis, N. Kousi, S. Makris, AR based robot programming using teaching by demonstration techniques, *Procedia CIRP* 97 (2021) 459–463, <http://dx.doi.org/10.1016/j.procir.2020.09.186>.
- [47] Y. Song, R. Koeck, A. Agkathidis, Augmented bricklayer: an augmented human-robot collaboration method for the robotic assembly of masonry structures, in: *XXVI International Conference of the Iberoamerican Society of Digital Graphics, Blucher*, 2023, pp. 713–724, http://dx.doi.org/10.5151/sigradi2022-sigradi2022_30.
- [48] C. Xue Er Shamaine, Y. Qiao, J. Henry, K. McNevin, N. Murray, RoSTAR: ROS-based teleoperated control via augmented reality, in: *2020 IEEE 22nd International Workshop on Multimedia Signal Processing, MMSP*, 2020, pp. 1–6, <http://dx.doi.org/10.1109/MMSP48831.2020.9287100>.
- [49] C. Vogel, C. Walter, N. Elkmann, Safeguarding and supporting future human-robot cooperative manufacturing processes by a projection- and camera-based technology, *Procedia Manuf.* 11 (2017) 39–46, <http://dx.doi.org/10.1016/j.promfg.2017.07.127>.
- [50] A. Hietanen, R. Pieters, M. Lanz, J. Latokartano, J.-K. Kämäräinen, AR-based interaction for human-robot collaborative manufacturing, *Robot. Comput.-Integr. Manuf.* 63 (2020) 101891, <http://dx.doi.org/10.1016/j.rcim.2019.101891>.
- [51] O. Kyjanek, B. Al Bahar, L. Vasey, B. Wannemacher, A. Menges, Implementation of an augmented reality AR workflow for human robot collaboration in timber prefabrication, in: *Proceedings of the 36th International Symposium on Automation and Robotics in Construction, ISARC*, 2019, pp. 1223–1230, <http://dx.doi.org/10.22260/ISARC2019/0164>.
- [52] I.X. Han, S. Parascho, Improv-structure: Exploring improvisation in collective human-robot construction, in: *Trends on Construction in the Digital Era*, Springer International Publishing, 2022, pp. 233–243, http://dx.doi.org/10.1007/978-3-031-20241-4_16.
- [53] Y. Song, R. Koeck, S. Luo, Review and analysis of augmented reality (AR) literature for digital fabrication in architecture, *Autom. Constr.* 128 (2021) 103762, <http://dx.doi.org/10.1016/j.autcon.2021.103762>.
- [54] G. Jahn, C. Newnham, N. van den Berg, Augmented reality for construction from steam-bent timber, in: *Proceedings of the 27th Conference on Computer Aided Architectural Design Research in Asia (CAADRIA)* [Volume 2], in: *CAADRIA 2022, CAADRIA*, 2022, <http://dx.doi.org/10.52842/conf.caadria.2022.2.191>.
- [55] H. Peng, J. Briggs, C.-Y. Wang, K. Guo, J. Kider, S. Mueller, P. Baudisch, F. Guimbretière, RoMA: Interactive fabrication with augmented reality and a robotic 3D printer, in: *Proceedings of the 2018 CHI Conference on Human Factors in Computing Systems, CHI '18, Association for Computing Machinery*, New York, NY, USA, 2018, pp. 1–12, <http://dx.doi.org/10.1145/3173574.3174153>.
- [56] C. Sun, Z. Zheng, T. Sun, Hybrid fabrication: a free-form building process with high on-site flexibility and acceptable accumulative error, in: *ACADIA Proceedings*, in: *ACADIA 2018, ACADIA*, 2018, <http://dx.doi.org/10.52842/conf.acadia.2018.082>.
- [57] J.-N.A. Dackiw, A. Foltman, S. Garivani, K. Kaseman, A. Sollazzo, Cyber-physical UAV navigation and operation, in: *Proceedings of the 39th Annual Conference of the Association for Computer Aided Design in Architecture, ACADIA*, in: *ACADIA 2019, ACADIA*, 2019, <http://dx.doi.org/10.52842/conf.acadia.2019.360>.
- [58] I.B. Alkan, H.B. Basaga, Augmented reality technologies in construction project assembly phases, *Autom. Constr.* 156 (2023) 105107, <http://dx.doi.org/10.1016/j.autcon.2023.105107>.
- [59] J. Alves, B. Marques, M. Oliveira, T. Araujo, P. Dias, B.S. Santos, Comparing spatial and mobile augmented reality for guiding assembling procedures with task validation, in: *2019 IEEE International Conference on Autonomous Robot Systems and Competitions, ICARSC*, IEEE, 2019, <http://dx.doi.org/10.1109/icarsc.2019.8733642>.
- [60] A. Plopski, T. Hirzle, N. Norouzi, L. Qian, G. Bruder, T. Langlotz, The eye in extended reality: A survey on gaze interaction and eye tracking in head-worn extended reality, *ACM Comput. Surv.* 55 (3) (2022) <http://dx.doi.org/10.1145/3491207>.
- [61] W.P. Chan, G. Hanks, M. Sakr, H. Zhang, T. Zuo, H.F.M. van der Loos, E. Croft, Design and evaluation of an augmented reality head-mounted display interface for human robot teams collaborating in physically shared manufacturing tasks, *J. Hum.- Robot. Interact.* 11 (3) (2022) <http://dx.doi.org/10.1145/3524082>.
- [62] Microsoft, HoloLens (1st gen) hardware, 2024, URL <https://learn.microsoft.com/en-us/hololens/hololens1-hardware>. (Accessed 18 December 2024).
- [63] Microsoft, About HoloLens 2, 2023, URL <https://learn.microsoft.com/en-us/hololens/hololens2-hardware>. (Accessed 18 December 2024).
- [64] A. Pose-Díez-de-la Lastra, R. Moreta-Martinez, M. García-Sevilla, D. García-Mato, J.A. Calvo-Haro, L. Mediavilla-Santos, R. Pérez-Mañanes, F. von Haxthausen, J. Pascau, HoloLens 1 vs. HoloLens 2: Improvements in the new model for orthopedic oncological interventions, *Sensors* 22 (13) (2022) <http://dx.doi.org/10.3390/s22134915>, URL <https://www.mdpi.com/1424-8220/22/13/4915>.
- [65] X. Yang, A. Sousa Calepso, F. Amtsberg, A. Menges, M. Sedlmair, Usability evaluation of an augmented reality system for collaborative fabrication between multiple humans and industrial robots, in: *Proceedings of the 2023 ACM Symposium on Spatial User Interaction, SUI '23, Association for Computing Machinery*, New York, NY, USA, 2023, <http://dx.doi.org/10.1145/3607822.3614528>.
- [66] L. Skouri, S. Treml, N. Opgenorth, F. Amtsberg, H.J. Wagner, A. Menges, T. Wortmann, Towards data-informed co-design in digital fabrication, *Autom. Constr.* 158 (2024) 105229, <http://dx.doi.org/10.1016/j.autcon.2023.105229>.
- [67] X. Yang, F. Amtsberg, L. Skouri, H.J. Wagner, A. Menges, Vizor, facilitating cyber-physical workflows in prefabrication through augmented reality, in: *Proceedings of the 27th Conference on Computer Aided Architectural Design Research in Asia (CAADRIA)* [Volume 2], in: *CAADRIA 2022, CAADRIA*, 2022, <http://dx.doi.org/10.52842/conf.caadria.2022.2.141>.
- [68] F. Amtsberg, X. Yang, L. Skouri, A. Sousa Calepso, M. Sedlmair, T. Wortmann, A. Menges, Multi-actor fabrication for digital timber construction, in: *eCAADe Proceedings*, in: *eCAADe 2023, eCAADe*, 2023, <http://dx.doi.org/10.52842/conf.ecaade.2023.1.417>.
- [69] L. Skouri, F. Amtsberg, X. Yang, H.J. Wagner, A. Menges, T. Wortmann, A framework for managing data in multi-actor fabrication processes, in: *Towards Radical Regeneration*, Springer International Publishing, 2022, pp. 601–615, http://dx.doi.org/10.1007/978-3-031-13249-0_47.
- [70] B. Kaiser, A. Reichle, A. Verl, Model-based automatic generation of digital twin models for the simulation of reconfigurable manufacturing systems for timber construction, *Procedia CIRP* 107 (2022) 387–392, <http://dx.doi.org/10.1016/j.procir.2022.04.063>, Leading manufacturing systems transformation – Proceedings of the 55th CIRP Conference on Manufacturing Systems 2022.

- [71] J. Frohm, V. Lindström, J. Stahre, M. Winroth, Levels of automation in manufacturing, *Ergon. - Int. J. Ergon. Hum. Factors* 30 (3) (2008) pp. 1–36, URL <https://api.semanticscholar.org/CorpusID:107745837>. (Accessed 18 December 2024).
- [72] F. Kannenberg, C. Zechmeister, M. Gil Pérez, Y. Guo, X. Yang, D. Forster, S. Hügle, P. Mindermann, M. Abdelaal, L. Balangé, V. Schweiger, D. Weiskopf, G.T. Gresser, P. Middendorf, M. Bischoff, J. Knippers, A. Menges, Toward reciprocal feedback between computational design, engineering, and fabrication to co-design coreless filament-wound structures, *J. Comput. Des. Eng.* 11 (3) (2024) 374–394, <http://dx.doi.org/10.1093/jcde/qwae048>.
- [73] K. AG, KUKA.SafeOperation, 2024, URL https://www.kuka.com/en-de/products/robot-systems/software/hub-technologies/kuka_safeoperation. (Accessed 24 July 2024).
- [74] I. S.p.A., The first safety radar sensor in the world with SIL2 certification for use in industrial safety applications, 2022, URL <https://www.inxpect.com/en/products/s101a/>. (Accessed 24 July 2024).
- [75] A. Kwilinski, M. Kardas, The role of the Pareto principle in quality management within industry 4.0: A comprehensive bibliometric analysis, *Virtual Econ.* 7 (3) (2024) [http://dx.doi.org/10.34021/ve.2024.07.03\(1\)](http://dx.doi.org/10.34021/ve.2024.07.03(1)).
- [76] J. Brooke, SUS: A quick and dirty usability scale, in: P.W. Jordan, B. Thomas, B. a. Weerdmeester, I.L. McClelland (Eds.), *Usability Evaluation in Industry*, Vol. 189, Taylor & Francis, London, 1996, pp. 189–194.
- [77] L. Goode, Microsoft's HoloLens 2 puts a full-fledged computer on your face, 2019, URL <https://www.wired.com/story/microsoft-hololens-2-headset/>. (Accessed 18 December 2024).
- [78] A.H. Kyaw, A.H. Xu, G. Jahn, N. van den Berg, C. Newnham, S. Zivkovic, Augmented reality for high precision fabrication of glued laminated timber beams, *Autom. Constr.* 152 (2023) 104912, <http://dx.doi.org/10.1016/j.autcon.2023.104912>.
- [79] A. Fazel, A. Adel, Enhancing construction accuracy, productivity, and safety with augmented reality for timber fastening, *Autom. Constr.* 166 (2024) 105596, <http://dx.doi.org/10.1016/j.autcon.2024.105596>.
- [80] P. Tsarouchi, S. Makris, G. Chryssolouris, Human–robot interaction review and challenges on task planning and programming, *Int. J. Comput. Integr. Manuf.* 29 (8) (2016) 916–931, <http://dx.doi.org/10.1080/0951192X.2015.1130251>.
- [81] Safety of Machinery — Safety-Related Parts of Control Systems, Standard, International Organization for Standardization, Geneva, CH, 2023, URL <https://www.iso.org/standard/73481.html>. (Accessed 24 July 2024).
- [82] Safety of Machinery - Functional Safety of Safety-Related Control Systems, Standard, International Electrotechnical Commission, Geneva, CH, 2021, URL <https://webstore.iec.ch/en/publication/71331>. (Accessed 24 July 2024).
- [83] D. Mitterberger, L. Atanasova, K. Dörfler, F. Gramazio, M. Kohler, Tie a knot: human–robot cooperative workflow for assembling wooden structures using rope joints, *Constr. Robot.* 6 (3–4) (2022) 277–292, <http://dx.doi.org/10.1007/s41693-022-00083-2>.
- [84] L. Skouri, T. Wortmann, Prediction models for co-design in industry 4.0, in: *Scalable Disruptors*, Springer Nature Switzerland, 2024, pp. 507–519, http://dx.doi.org/10.1007/978-3-031-68275-9_41.
- [85] E. Ruschel, E.d.F. Rocha Loures, E.A.P. Santos, Performance analysis and time prediction in manufacturing systems, *Comput. Ind. Eng.* 151 (2021) 106972, <http://dx.doi.org/10.1016/j.cie.2020.106972>.
- [86] Y. Rogers, P. Marshall, *Research in the Wild*, Morgan & Claypool Publishers, 2017, <http://dx.doi.org/10.1007/978-3-031-02220-3>.
- [87] H. Li, W. Ma, H. Wang, G. Liu, X. Wen, Y. Zhang, M. Yang, G. Luo, G. Xie, C. Sun, A framework and method for human–robot cooperative safe control based on digital twin, *Adv. Eng. Inform.* 53 (2022) 101701, <http://dx.doi.org/10.1016/j.aei.2022.101701>.
- [88] S. Yi, S. Liu, Y. Yang, S. Yan, D. Guo, X.V. Wang, L. Wang, Safety-aware human-centric collaborative assembly, *Adv. Eng. Inform.* 60 (2024) 102371, <http://dx.doi.org/10.1016/j.aei.2024.102371>.
- [89] G. Schirner, D. Erdogan, K. Chowdhury, T. Padir, The future of human-in-the-loop cyber-physical systems, *Computer* 46 (1) (2013) 36–45, <http://dx.doi.org/10.1109/MC.2013.31>.
- [90] H. Limerick, D. Coyle, J.W. Moore, The experience of agency in human-computer interactions: a review, *Front. Hum. Neurosci.* 8 (2014) <http://dx.doi.org/10.3389/fnhum.2014.00643>.
- [91] X. Yang, P. Sasikumar, F. Amtsberg, A. Menges, M. Sedlmair, S. Nanayakkara, Who is in control? Understanding user agency in AR-assisted construction assembly, in: Proceedings of the 2025 CHI Conference on Human Factors in Computing Systems, CHI '25, Association for Computing Machinery, New York, NY, USA, 2025, <http://dx.doi.org/10.1145/3706598.3713765>.